

# Synthesis of Enantiopure Iridium(I) and Iridium(III) Pybox Complexes and Their Application in the Asymmetric Transfer Hydrogenation of Ketones<sup>†</sup>

Paloma Paredes, Josefina Díez, and M. Pilar Gamasa\*

Instituto Universitario de Química Organometálica “Enrique Moles” (Unidad Asociada al CSIC),  
Departamento de Química Orgánica e Inorgánica, Facultad de Química, Universidad de Oviedo,  
33071 Oviedo, Spain

Received November 28, 2007

Iridium(III) complexes have been obtained from the complexes  $[\text{Ir}(\eta^2\text{-C}_2\text{H}_4)_2(\kappa^3\text{-N,N,N-R-pybox})][\text{PF}_6]$  or from  $[\text{Ir}(\mu\text{-Cl})(\eta^2\text{-C}_8\text{H}_{14})_2]_2$  and R-pybox mixtures by oxidative addition reactions. The treatment of complexes  $[\text{Ir}(\eta^2\text{-C}_2\text{H}_4)_2(\kappa^3\text{-N,N,N-R-pybox})][\text{PF}_6]$  (R-pybox = 2,6-bis[4'-(S)-isopropylloxazolin-2'-yl]pyridine (**1**), 2,6-bis[4'-(R)-phenyloxazolin-2'-yl]pyridine (**2**)) with HCl, I<sub>2</sub>, and allyl chloride under mild conditions results in most cases in the stereoselective formation of the iridium(III) complexes  $[\text{IrClH}(\eta^2\text{-C}_2\text{H}_4)(\kappa^3\text{-N,N,N-R-pybox})][\text{PF}_6]$  (R = <sup>i</sup>Pr (**4**), Ph (**5**)),  $[\text{IrI}_2(\eta^2\text{-C}_2\text{H}_4)(\kappa^3\text{-N,N,N-R-pybox})][\text{PF}_6]$  (R = <sup>i</sup>Pr (**8**), Ph (**9**)), and  $[\text{IrCl}(\eta^3\text{-C}_3\text{H}_5)(\kappa^3\text{-N,N,N-R-pybox})][\text{PF}_6]$  (R = <sup>i</sup>Pr (**10**), Ph (**11**)). The substitution of ethylene by acetonitrile in **4** and **5** affords the complexes  $[\text{IrClH}(\text{MeCN})(\kappa^3\text{-N,N,N-R-pybox})][\text{PF}_6]$  (R = <sup>i</sup>Pr (**6**), Ph (**7**)). Neutral iridium(III) complexes  $[\text{IrCl}_3(\kappa^3\text{-N,N,N-R-pybox})]$  (R-pybox = <sup>i</sup>Pr (**12**), Ph (**13**)) have been prepared in high yield by reaction of the complex  $[\text{Ir}(\mu\text{-Cl})(\eta^2\text{-C}_8\text{H}_{14})_2]_2$  with chlorine and R-pybox in dichloromethane at room temperature. The reaction of **12** or **13** in acetone with silver or thallium salts of poorly coordinating anions, e.g., AgBF<sub>4</sub>, AgSbF<sub>6</sub>, or TlPF<sub>6</sub>, at room temperature gives the complexes  $[\text{IrCl}_2(\kappa^3\text{-N,N,N-R-pybox})(\mu\text{-Cl})\text{M}][\text{Y}]$  (R = <sup>i</sup>Pr, M = Ag, Y = BF<sub>4</sub> (**14a**), SbF<sub>6</sub> (**14b**), M = Tl, X = PF<sub>6</sub> (**14c**); R = Ph, M = Ag, Y = BF<sub>4</sub> (**15a**), SbF<sub>6</sub> (**15b**), M = Tl, Y = PF<sub>6</sub> (**15c**)). The structures of derivatives **1**, **8**, **10**, and **14c** have been determined by single-crystal X-ray diffraction analysis. The complexes **1**, **2**, **4**–**6**, **8**, **10**, **12**, **13**, and **14a**–**c** and the previously reported  $[\text{Ir}(\eta^2\text{-C}_2\text{H}_4)_2(\kappa^3\text{-N,N,N-Ph-pybox})][\text{PF}_6]$  (**3**) and  $[\text{IrClH}(\text{CO})(\kappa^3\text{-N,N,N-Ph-pybox})][\text{PF}_6]$  have been assayed as catalysts for the asymmetric transfer hydrogenation of ketones. The <sup>i</sup>Pr-pybox-iridium(III) complexes **4**, **6**, **12**, and **14a** are shown to be more efficient catalysts, with high conversions and ee up to 77%.

## Introduction

Asymmetric synthesis catalyzed by transition metal complexes bearing enantiopure pybox as ancillary ligands has experienced a pronounced growth in recent years.<sup>1</sup> Having in mind the great importance of iridium complexes in catalytic processes, it is remarkable that (i) the coordination chemistry of pybox–iridium metal remains unexplored and (ii) only a few examples of asymmetric catalysis using the  $[\text{Ir}(\mu\text{-Cl})(\text{cod})]_2/\text{pybox}$  combination as the catalyst have been hitherto reported. Thus, the first study on the synthesis of iridium–pybox complexes has been recently described from our laboratory,<sup>2</sup> while the  $[\text{Ir}(\mu\text{-Cl})(\text{cod})]_2/\text{indane-pybox}$ -catalyzed reductive aldol reaction<sup>3</sup> and the enantioselective allylic substitution with nitrogen nucleophiles catalyzed by mixtures of  $[\text{Ir}(\mu\text{-Cl})(\text{cod})]_2/$

phenyl–pybox<sup>4</sup> have been published by Morken and Takemoto, respectively.

As part of our ongoing research dealing with groups 8, 9, and 11 metal complexes bearing enantiopure pybox ligands,<sup>2,5</sup> we report herein the synthesis of iridium(I) and iridium(III) complexes containing the (S,S)-<sup>i</sup>Pr-pybox and (R,R)-Ph-pybox ligands as well as their application in asymmetric transfer hydrogenation of ketones. As far as we are aware, a sole example dealing with the use of pybox–metal complexes in transfer hydrogenation of prochiral ketones has been reported. Specifically, a variety of aromatic ketones have been reduced to the secondary alcohols by the ruthenium complexes *trans*- and *cis*- $[\text{RuCl}_2(\text{L})\{\kappa^3\text{-N,N,N-(R,R)-Ph-pybox}\}]$  (L = phosphine or phosphite) with up to 94% ee and very high TOF.<sup>5b</sup>

<sup>†</sup> Dedicated to Professor José Gimeno on the occasion of his 60th birthday.

\* Corresponding author. Fax: (internat.) 34-985103446. E-mail: pgb@uniovi.es.

(1) Desimoni, G.; Faita, G.; Quadrelli, P. *Chem. Rev.* **2003**, *103*, 3119–3154.

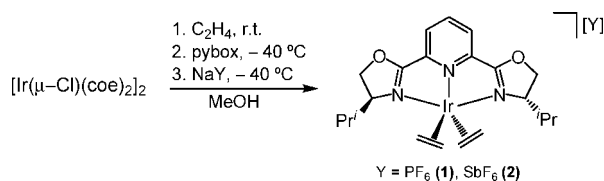
(2) (a) Díez, J.; Gamasa, M. P.; Gimeno, J.; Paredes, P. *Organometallics* **2005**, *24*, 1799–1802. (b) Cuervo, D.; Díez, J.; Gamasa, M. P.; Gimeno, J.; Paredes, P. *Eur. J. Inorg. Chem.* **2006**, 599–608.

(3) Zhao, C.-X.; Duffey, M. O.; Taylor, S. J.; Morken, J. P. *Org. Lett.* **2001**, *3*, 1829–1831.

(4) (a) Miyabe, H.; Matsumura, A.; Motiyama, K.; Takemoto, Y. *Org. Lett.* **2004**, *6*, 4631–4634. (b) Miyabe, H.; Yoshida, K.; Yamauchi, M.; Takemoto, Y. *J. Org. Chem.* **2005**, *70*, 2148–2153. (c) Review: Miyabe, H.; Takemoto, Y. *Synlett* **2005**, 1641–1655.

(5) Ruthenium(II): (a) Cadierno, V.; Gamasa, M. P.; Gimeno, J.; Iglesias, L.; García-Granda, S. *Inorg. Chem.* **1999**, *38*, 2874–2879. (b) Cuervo, D.; Gamasa, M. P.; Gimeno, J. *Chem.–Eur. J.* **2004**, *10*, 425–432. Rhodium(I) and rhodium(III): (c) Cuervo, D.; Díez, J.; Gamasa, M. P.; García-Granda, S.; Gimeno, J. *Inorg. Chem.* **2002**, *41*, 4999–5001. (d) Cuervo, D.; Díez, J.; Gamasa, M. P.; Gimeno, J. *Organometallics* **2005**, *23*, 2224–2232. (e) Cuervo, D.; Gamasa, M. P.; Gimeno, J. *J. Mol. Catal. A: Chem.* **2006**, *249*, 60–64. (f) Copper(I): Díez, J.; Gamasa, M. P.; Panera, M. *Inorg. Chem.* **2006**, *45*, 10043–10045.

Scheme 1



## Results and Discussion

**Synthesis of the Complexes  $[\text{Ir}(\eta^2\text{-C}_2\text{H}_4)_2\{\kappa^3\text{-N,N,N-(S,S)-iPr-pybox}\}][\text{Y}]$  ( $\text{Y} = \text{PF}_6\text{ (1)}, \text{SbF}_6\text{ (2)}$ ).** The reaction of the complex  $[\text{Ir}(\mu\text{-Cl})(\eta^2\text{-C}_8\text{H}_{14})_2]_2$  ( $\text{C}_8\text{H}_{14}$  = cyclooctene) with ethylene (1 atm) in methanol at room temperature followed by successive addition of  $i\text{Pr-pybox}$  ( $i\text{Pr-pybox}$  = 2,6-bis[4'-(*S*)-isopropylloxazolin-2'-yl]pyridine) (2 equiv,  $-40\text{ }^\circ\text{C}$ ) and NaY ( $\text{Y} = \text{PF}_6, \text{SbF}_6$ ) gives rise, after workup, to the complexes  $[\text{Ir}(\eta^2\text{-C}_2\text{H}_4)_2\{\kappa^3\text{-N,N,N-(S,S)-iPr-pybox}\}][\text{Y}]$  ( $\text{Y} = \text{PF}_6\text{ (1)}, \text{SbF}_6\text{ (2)}$ ) as air-stable orange solids in excellent yield (94–95%) (Scheme 1). The NMR data of **1** and **2** reveal the presence of a  $\text{C}_2$  symmetry axis. A broad singlet at 2.89 ppm and a singlet at ca. 32.0 ppm, assigned to the hydrogen and carbon atoms of the ethylene ligand, are the most significant spectroscopic features for compounds **1** and **2**. These data are consistent with a fast rotation of the olefin ligands around their respective metal–ligand axes at room temperature on the NMR time scale. Variable-temperature  $^1\text{H}$  NMR studies (291–183 K) carried out for complex **1** clearly support the dynamic behavior of the olefin ligand in the complexes.<sup>2a</sup>

The structure of complex **1** has been confirmed by a single-crystal X-ray analysis. An ORTEP-type view of the cation complex is shown in Figure 1, and selected bonding data are collected in the caption. For further structural data see ref 2a.

Since oxidative addition steps are frequently proposed in catalytic cycles, we have investigated the stability of the

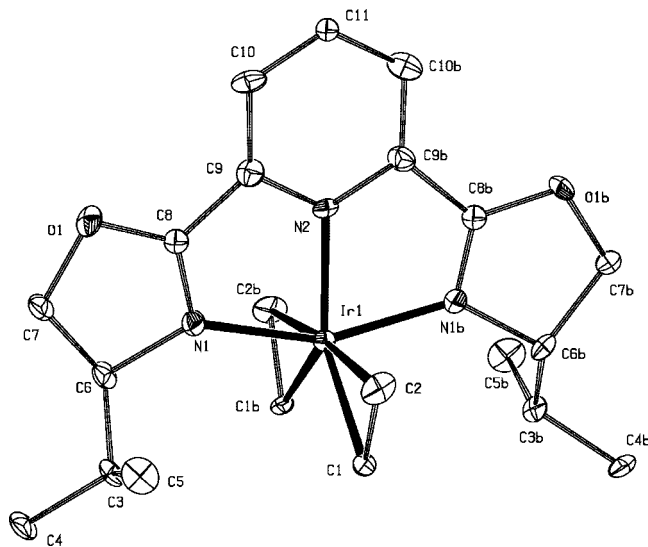
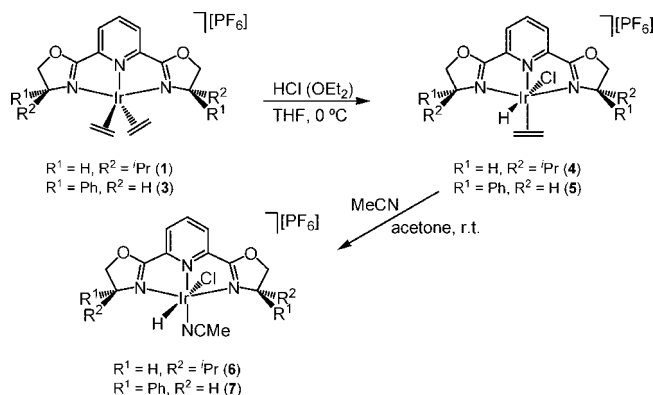


**Figure 1.** ORTEP-type view of the molecular structure of the cation of  $[\text{Ir}(\eta^2\text{-C}_2\text{H}_4)_2\{\kappa^3\text{-N,N,N-(S,S)-iPr-pybox}\}][\text{PF}_6]$  (**1**) showing atom-labeling scheme. Atoms labeled with an “b” are related to those indicated by a crystallographic  $\text{C}_2$  symmetry axis. Thermal ellipsoids are drawn at 30% probability. Hydrogen atoms have been omitted for clarity. Selected bond lengths (Å) and angles (deg): Ir–N(1), 2.041(10); Ir–N(2), 2.015(10); Ir–C(1), 2.138(12); Ir–C(2), 2.104(14); C(1)–C(2), 1.414(16); Ir–CT01, 2.0089(1); N(2)–Ir–N(1), 77.8(3); N(2)–Ir–C(1), 132.3(3); N(2)–Ir–C(2), 93.4(4); N(2)–Ir–CT01, 113.01; CT01 = midpoint of C(1)–C(2) bond length.

Scheme 2



complexes  $[\text{Ir}(\eta^2\text{-C}_2\text{H}_4)_2\{\kappa^3\text{-N,N,N-(S,S)-iPr-pybox}\}][\text{PF}_6]$  (**1**) and  $[\text{Ir}(\eta^2\text{-C}_2\text{H}_4)_2\{\kappa^3\text{-N,N,N-(R,R)-Ph-pybox}\}][\text{PF}_6]$  (**3**),<sup>2b</sup> as well as that of  $[\text{Ir}(\mu\text{-Cl})(\eta^2\text{-C}_8\text{H}_{14})_2]_2/\text{pybox}$  mixtures, in processes of this type. Herein, cationic and neutral complexes with a range of ligands to complete the coordination sphere around the iridium center are reported.

**1. Synthesis of Iridium(III) Complexes by Stereoselective Oxidative Addition to the Bis(ethylene) Iridium(I)  $[\text{Ir}(\eta^2\text{-C}_2\text{H}_4)_2(\kappa^3\text{-N,N,N-R-pybox})][\text{PF}_6]$  ( $\text{R} = (\text{S,S})\text{-iPr (1)}, (\text{R,R})\text{-Ph (3)}$ ) Complexes.** We are particularly interested in the synthesis of hydride and allyl complexes, a type of species that are extensively found as intermediates in both stoichiometric and catalytic processes. In particular, monohydride iridium complexes have been proposed as active species in catalytic transfer hydrogenation of ketones.<sup>6</sup>

**1.a. Synthesis of Hydride Complexes  $[\text{IrClH}(\eta^2\text{-C}_2\text{H}_4)(\kappa^3\text{-N,N,N-R-pybox})][\text{PF}_6]$  ( $\text{R} = i\text{Pr (4)}, \text{Ph (5)}$ ) and  $[\text{IrClH}(\text{MeCN})(\kappa^3\text{-N,N,N-R-pybox})][\text{PF}_6]$  ( $\text{R} = i\text{Pr (6)}, \text{Ph (7)}$ ).** The treatment of a solution of complexes  $[\text{Ir}(\eta^2\text{-C}_2\text{H}_4)_2\{\kappa^3\text{-N,N,N-(S,S)-iPr-pybox}\}][\text{PF}_6]$  (**1**) or  $[\text{Ir}(\eta^2\text{-C}_2\text{H}_4)_2\{\kappa^3\text{-N,N,N-(R,R)-Ph-pybox}\}][\text{PF}_6]$  (**3**)<sup>2b</sup> in THF with a solution of HCl in diethyl ether at  $0\text{ }^\circ\text{C}$  results in the stereoselective formation of the complexes  $[\text{IrClH}(\eta^2\text{-C}_2\text{H}_4)(\kappa^3\text{-N,N,N-R-pybox})][\text{PF}_6]$  ( $\text{R} = i\text{Pr (4)}, \text{Ph (5)}$ ) isolated as yellow solids in 88–94% yield. The synthesis of complex **4** has been previously communicated.<sup>2a</sup> Moreover, the addition of acetonitrile to an acetone solution of complexes **4** and **5** at  $0\text{ }^\circ\text{C}$  followed by warming to room temperature allows for the ethylene–acetonitrile ligand exchange, affording the complexes **6** and **7**, which are isolated as orange air-stable solids in high yield (84–86%) (Scheme 2).

Complexes **4–7** have been characterized by elemental analyses, molar conductivity, mass spectra (FAB) (complexes **5, 6**), and NMR spectroscopy (see Experimental Section for details). The  $^{13}\text{C}$  NMR spectra of complexes **4** and **5** were taken at 233 K because of slow decomposition at higher temperature. Significant spectroscopic data features are (a) the characteristic  $\nu(\text{Ir–H})$  IR absorption observed at 2186 (**4**), 2173 (**5**), 2160 (**6**), and  $2165\text{ cm}^{-1}$  (**7**); (b) the high-field singlet signal for the hydride ligand in the  $^1\text{H}$  NMR spectra that appears in the range  $-22.56$  to  $-24.93$  ppm; (c) the NMR resonances for the ethylene group in complexes **4** and **5** (a multiplet at 4.77 ppm (**4**) and two multiplets at 3.83, 3.45 ppm (**5**) in the  $^1\text{H}$  NMR spectra as well as a singlet at ca. 60.0 ppm (**4** and **5**) in the  $^{13}\text{C}\{^1\text{H}\}$  NMR spectra); and (d) the resonance of the

(b) (a) Pàmies, O.; Bäckvall, J.-E. *Chem. – Eur. J.* **2001**, *7*, 5052–5057. (b) Computational studies Ru/Ir: Handgraaf, J.-W.; Reek, J. N. H.; Meijer, E. J. *Organometallics* **2003**, *22*, 3150–3157. (c) Samec, J. S. M.; Bäckvall, J.-E.; Andersson, P. G.; Brandt, P. *Chem. Soc. Rev.* **2006**, *35*, 237–248.

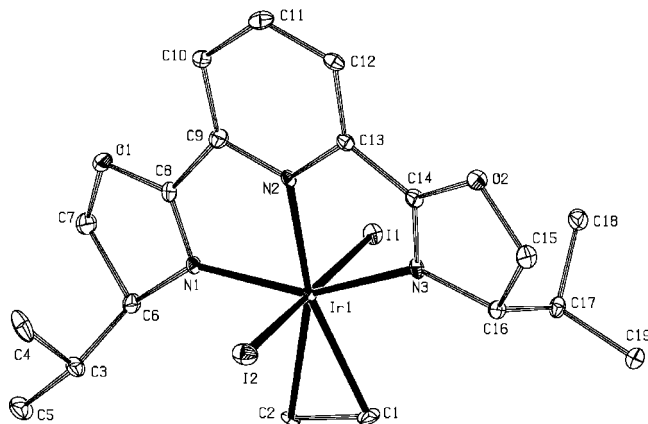
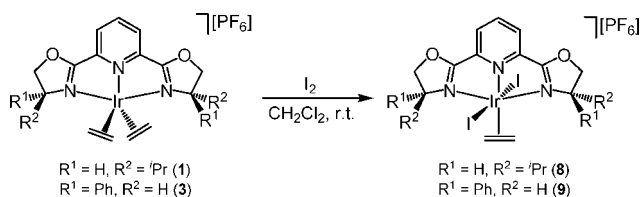


**Figure 2.** ORTEP-type view of the molecular structure of the cation of  $[\text{IrI}_2(\eta^2\text{-C}_2\text{H}_4)_2\{\kappa^3\text{-N,N,N-(S,S)-iPr-pybox}\}][\text{PF}_6]$  (**8**) showing atom-labeling scheme. Thermal ellipsoids are drawn at 20% probability. Hydrogen atoms have been omitted for clarity.

**Scheme 3**



acetonitrile ligand in complexes **6** and **7** in the ranges 3.02–1.84 ppm ( $^1\text{H}$  NMR) and 124.0–121.0 and 3.6–1.8 ppm ( $^{13}\text{C}\{^1\text{H}\}$  NMR).

Although three stereoisomers can be formed, a single reaction product was in all cases observed according to the NMR and IR spectroscopic data. Unfortunately, an X-ray analysis to determine the stereoisomer obtained could not be performed since all attempts to crystallize complexes **4**–**7** have been unsuccessful. We assume that the hydride and chlorine ligands in complexes **4** and **5** are *trans* to each other, in a similar stereochemical environment to that found for complex **8** (see Figure 2) and for  $[\text{IrCl}(\text{CH}_3)(\text{CO})(\kappa^3\text{-N,N,N-}i\text{Pr-pybox})][\text{PF}_6]$ , whose structure was proven by X-ray diffraction analysis.<sup>2b</sup> Moreover, we propose that complexes **6** and **7**, formed by ligand exchange from complexes **4** and **5**, present the same stereochemical arrangement as their precursors, the acetonitrile ligand being placed *trans* to the pyridine nitrogen of the pybox ligand.

**1.b. Synthesis of Complexes  $[\text{IrI}_2(\eta^2\text{-C}_2\text{H}_4)_2(\kappa^3\text{-N,N,N-R-pybox})][\text{PF}_6]$  (**R** = *i*Pr (**8**), Ph (**9**)).** The reaction of equimolecular amounts of complexes  $[\text{Ir}(\eta^2\text{-C}_2\text{H}_4)_2(\kappa^3\text{-N,N,N-R-pybox})][\text{PF}_6]$  (**R** = *i*Pr (**1**), Ph (**3**)) and iodine in dichloromethane at room temperature produces the iridium(III) complexes  $[\text{IrI}_2(\eta^2\text{-C}_2\text{H}_4)_2(\kappa^3\text{-N,N,N-R-pybox})][\text{PF}_6]$  (**R** = *i*Pr (**8**), Ph (**9**)) in a stereoselective manner (Scheme 3). The complexes have been isolated as air-stable red-brown (**8**) or yellow (**9**) solids (86% and 89% yield, respectively) and characterized by elemental analyses, molar conductivity, mass spectra (FAB) (compound **8**), and NMR spectroscopy (see Experimental Section for details). The spectroscopic NMR data of **8** and **9** are consistent with the presence of a  $\text{C}_2$  symmetry axis, indicating a *trans* arrangement for the iodine atoms.<sup>7</sup> Charac-

**Table 1.** Selected Bond Distances (Å) and Angles (deg) for Complex **8**

bond	distance	bond	distance
Ir–N(2)	2.004(5)	I(2)–Ir	2.652(5)
Ir–N(1)	2.068(5)	C(1)–Ir	2.215(7)
Ir–N(3)	2.068(5)	C(2)–Ir	2.216(6)
I(1)–Ir	2.678(5)	C(1)–C(2)	1.352(10)
angle	value	angle	value
I(2)–Ir–I(1)	179.52(2)	N(2)–Ir–N(3)	77.1(2)
N(3)–Ir–I(2)	87.87(15)	N(1)–Ir–N(3)	154.0(2)
N(2)–Ir–I(2)	89.00(15)	N(2)–Ir–N(1)	76.9(2)
N(1)–Ir–I(2)	93.33(15)	N(2)–Ir–C(1)	162.2(2)
N(3)–Ir–I(1)	92.60(15)	N(2)–Ir–C(2)	162.2(2)
N(2)–Ir–I(1)	91.10(15)	C(1)–Ir–C(2)	35.5(3)
N(1)–Ir–I(1)	86.25(15)	C(2)–C(1)–Ir	72.3(4)
N(2)–Ir–N(1)	76.9(2)	C(1)–C(2)–Ir	72.2(4)

teristic NMR resonances for the ethylene group: (a)  $^1\text{H}$  NMR spectra: two multiplets at 6.21 and 5.91 ppm (for complex **8**) and a multiplet at 5.86 ppm (for complex **9**); (b)  $^{13}\text{C}\{^1\text{H}\}$  NMR spectra: a singlet signal at 71.3 and 70.6 ppm for compounds **8** and **9**, respectively.

An X-ray crystal structure analysis has been performed for complex **8**. An ORTEP-type view of the cation complex is shown in Figure 2, and selected bonding data are listed in Table 1. The structure shows the expected distorted octahedral coordination of the iridium atom. The metal is bonded to two *trans*-oriented iodine atoms, to three pybox nitrogen atoms, and to the olefin that formally is occupying a coordination site (Figure 2). The carbon–carbon bond length in the ethylene ligand as well as the iridium–carbon bond lengths can be compared with those found in the case of complex **1**. While the olefin C(1)–C(2) bond length in complex **8** (1.352(10) Å) is slightly shorter than that found in complex **1** (1.414(16) Å), the Ir–C(1) and Ir–C(2) bond lengths are slightly longer in complex **8** than in complex **1** (2.215(7) versus 2.138(12) Å and 2.216(6) versus 2.104(14) Å, respectively). The C(1)–C(2) bond length is in the same range as found in other olefin iridium(I) complexes.<sup>8</sup> The N(1)–Ir–N(3) angle (154.0(2)°) and the Ir–N(2) (2.004(5) Å), Ir–N(1) (2.068(5) Å), and Ir–N(3) (2.068(5) Å) bond lengths are similar to those found in complexes **1** and **10**.

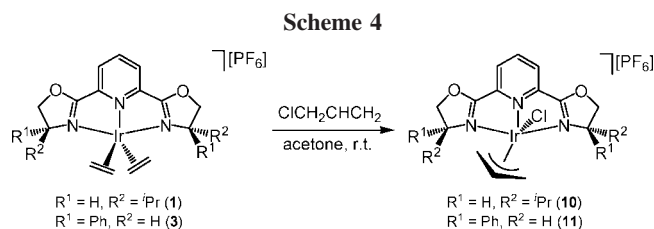
**1.c. Synthesis of Complexes  $[\text{IrCl}(\eta^3\text{-C}_3\text{H}_5)(\kappa^3\text{-N,N,N-R-pybox})][\text{PF}_6]$  (**R** = *i*Pr (**10**), Ph (**11**)).** The reaction of the complexes  $[\text{Ir}(\eta^2\text{-C}_2\text{H}_4)_2(\kappa^3\text{-N,N,N-R-pybox})][\text{PF}_6]$  (**R** = *i*Pr (**1**), Ph (**3**)) with allyl chloride (1:1.5 molar ratio) in acetone at room temperature yields the complexes  $[\text{IrCl}(\eta^3\text{-C}_3\text{H}_5)(\kappa^3\text{-N,N,N-R-pybox})][\text{PF}_6]$  (**R** = *i*Pr (**10**), Ph (**11**)). According to the  $^{13}\text{C}\{^1\text{H}\}$  NMR spectra of the reaction crude complex **10** is formed as a single diastereoisomer and a 2:1 diastereoisomeric mixture is obtained for complex **11**. These complexes have been isolated as air-stable yellow solids in 84–93% yield (Scheme 4). Their analytical and spectroscopic data ( $^1\text{H}$  and  $^{13}\text{C}\{^1\text{H}\}$  NMR and IR) are in full agreement with the proposed formulations. The  $^1\text{H}$  and  $^{13}\text{C}\{^1\text{H}\}$  NMR spectra of both complexes at room temperature are in accordance with the presence of a rigid allyl group structure in solution (see Experimental Section for details).

The stereochemistry of complex **10** has been confirmed by a single-crystal X-ray analysis. An ORTEP-type view of the cation complex, along with the more significant bond length and angle

(7) The pattern of  $^1\text{H}$  and  $^{13}\text{C}\{^1\text{H}\}$  NMR spectra of pybox ligands provides an unequivocal structural elucidation in *cis* or *trans* dihalogen octahedral complexes containing pybox ligands. See for example *cis*- and *trans*- $[\text{RuCl}_2(\text{L})(\text{Ph-pybox})]$  (L = phosphine) (ref 5b) and *trans*- $[\text{M}(\text{CO})(\text{Pr-pybox})][\text{PF}_6]$  (M = Rh, Ir) (ref 2b).

(8) (a) Alvarado, Y.; Boutry, O.; Gutiérrez, E.; Monge, A.; Nicasio, M. C.; Poveda, M. L.; Pérez, P. J.; Rufz, C.; Bianchini, C.; Carmona, E. *Chem.-Eur. J.* **1997**, *3*, 860–873. (b) Lundquist, E. G.; Folting, K.; Streib, W. E.; Huffman, J. C.; Eisenstein, O.; Caulton, K. G. *J. Am. Chem. Soc.* **1990**, *112*, 855–863.

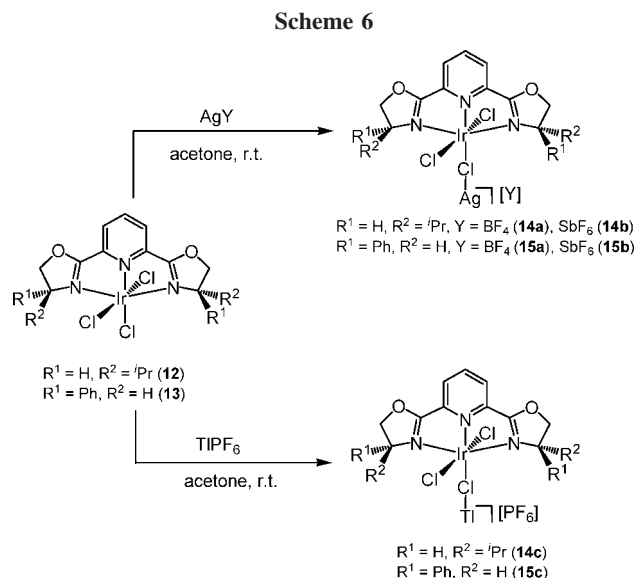
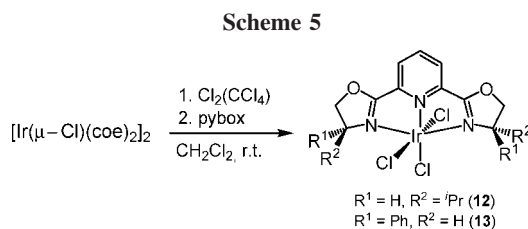




values, is shown in Figure 3. For further structural data see ref 2a. We assumed that the stereochemistry of complex **10** is maintained in the major isomer of complex **11**.

The reaction presumably involves the formation of a non-detected monoolefin iridium(III) complex intermediate in which the allyl group participates as a monodentate ligand. This  $\eta^1$ -coordination type of allyl group has been recently found in the complexes  $[\text{IrCl}(\eta^1\text{-CH}_2\text{CHCH}_2)(\text{CO})(\kappa^3\text{-}N,N,N\text{-}R\text{-pybox})][\text{PF}_6]$  ( $R = i\text{Pr}, \text{Ph}$ )<sup>2b</sup> formed from complexes  $[\text{Ir}(\text{CO})(\kappa^3\text{-}N,N,N\text{-}R\text{-pybox})][\text{PF}_6]$  and allyl chloride. These monocarbonyl complexes do not evolve into the corresponding  $\eta^3$ -allyl complexes by loss of carbon monoxide.

**2. Synthesis of Iridium(III) Complexes by Oxidative Addition of Chlorine to  $[\text{Ir}(\mu\text{-Cl})(\eta^2\text{-C}_8\text{H}_{14})_2]/\text{pybox}$  Mixtures: Synthesis of Complexes  $[\text{IrCl}_3(\kappa^3\text{-}N,N,N\text{-}R\text{-pybox})]$  ( $R = i\text{Pr}$  (**12**),  $\text{Ph}$  (**13**)).** The treatment of a suspension of  $[\text{Ir}(\mu\text{-Cl})(\eta^2\text{-C}_8\text{H}_{14})_2]$  in dichloromethane with a saturated solution of chlorine in  $\text{CCl}_4$  and pybox at room temperature affords the complexes  $[\text{IrCl}_3(\kappa^3\text{-}N,N,N\text{-}R\text{-pybox})][\text{PF}_6]$  ( $R = i\text{Pr}$  (**12**),  $\text{Ph}$  (**13**)) as dark green or yellow air-stable solids in good yields (76–78%) (Scheme 5). Their analytical, mass spectrum (ESI) (complex **12**), and spectroscopic ( $^1\text{H}$ ,  $^{13}\text{C}\{^1\text{H}\}$  NMR) data support the proposed formulations (see Experimental Section for details). Conductivity measurements in acetone confirm the neutral character of complexes **12** and **13** in solution and rule out the participation of the ion pair  $[\text{IrCl}_2(\kappa^3\text{-}N,N,N\text{-}R\text{-pybox})][\text{Cl}]$  by halide dissociation. The spectroscopic NMR data for **12** and **13** are consistent with the presence of a  $C_2$  symmetry



axis. These derivatives are structurally analogous to the  $[\text{RhCl}_3(R\text{-pybox})]$  complexes reported by Nishiyama in his pioneering catalytic hydrosilylation reaction of ketones.<sup>9</sup> Unfortunately, an X-ray analysis could not be performed since all attempts to crystallize complexes **12** and **13** have been unsuccessful.

**3. Reactivity of Complexes  $[\text{IrCl}_3(\kappa^3\text{-}N,N,N\text{-}R\text{-pybox})]$  ( $R = i\text{Pr}$  (**12**),  $\text{Ph}$  (**13**)) with Silver and Thallium Salts  $[\text{AgY}]$  ( $\text{Y} = \text{BF}_4, \text{SbF}_6$ ),  $\text{TlPF}_6$ ]: Synthesis of the Complexes  $[\text{IrCl}_2(\kappa^3\text{-}N,N,N\text{-}R\text{-pybox})(\mu\text{-Cl})\text{M}][\text{Y}]$  ( $R = i\text{Pr}$ ,  $\text{M} = \text{Ag}$ ,  $\text{Y} = \text{BF}_4$  (**14a**),  $\text{SbF}_6$  (**14b**),  $\text{M} = \text{Tl}$ ,  $\text{Y} = \text{PF}_6$  (**14c**);  $R = \text{Ph}$ ,  $\text{M} = \text{Ag}$ ,  $\text{Y} = \text{BF}_4$  (**15a**),  $\text{SbF}_6$  (**15b**),  $\text{M} = \text{Tl}$ ,  $\text{Y} = \text{PF}_6$  (**15c**)).** Halide abstraction using silver salts is a common method to generate transition metal complexes with coordinate anions or cationic-solvent coordinate complexes. However, compounds containing a  $[\text{M}-\text{X}-\text{Ag}]$  ( $\text{X} = \text{Cl}, \text{Br}, \text{I}$ ) linkage have been isolated in some cases.<sup>10</sup> In the present study, this type of reactivity is reported for complexes **12** and **13** by using  $\text{AgBF}_4$  as the halide abstracting agent. Thus, the reaction of complexes **12** and **13** with  $\text{AgBF}_4$  (1:2 molar ratio) provides the complexes **14a** and **15a** as red solids (94–96%) without precipitation of  $\text{AgCl}$  (Scheme 6). These derivatives are soluble in acetone and insoluble in diethyl ether and hexane and have been fully characterized by elemental analyses, mass spectra (ESI), and IR and NMR ( $^1\text{H}$ ,  $^{13}\text{C}\{^1\text{H}\}$ ) spectroscopy. The NMR data for **14a** and **15a** are consistent with the presence of a  $C_2$  symmetry axis. The IR spectra show the characteristic absorption band of

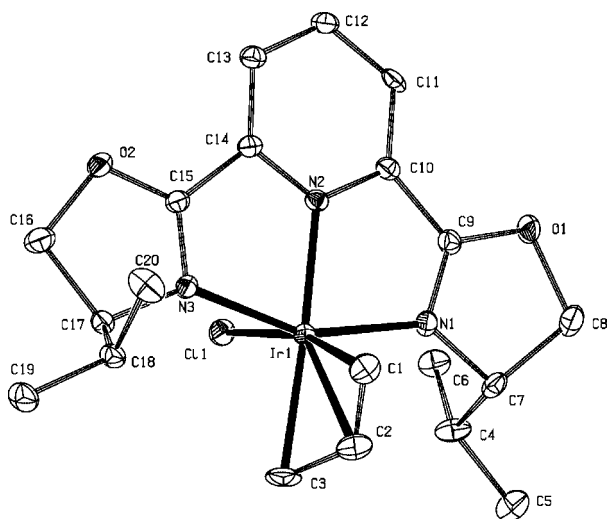


**Figure 3.** ORTEP-type view of the molecular structure of the cation of  $[\text{IrCl}(\eta^3\text{-C}_3\text{H}_5)\{\kappa^3\text{-}N,N,N\text{-}(S,S)\text{-}i\text{Pr-pybox}\}][\text{PF}_6]$  (**10**) showing atom-labeling scheme. Thermal ellipsoids are drawn at 10% probability. Hydrogen atoms have been omitted for clarity. Selected bond lengths (Å) and angles (deg): Ir–N(1), 2.063(6); Ir–N(2), 2.018(5); Ir–N(3), 2.071(5); Ir–Cl(1), 2.4223(18); Ir–C(1), 2.139(7); Ir–C(2), 2.119(8); Ir–C(3), 2.207(8); C(1)–C(2), 1.42(2); C(2)–C(3), 1.282(15); N(2)–Ir–N(1), 77.5(2); N(2)–Ir–N(3), 78.1(2); N(1)–Ir–N(3), 155.6(2); Cl(1)–Ir–C(1), 165.9(4); N(2)–Ir–C(3), 173.5(3); N(3)–Ir–C(1), 94.5(4); N(1)–Ir–C(1), 93.1(3).

(9) (a) Nishiyama, H.; Sakaguchi, H.; Nakamura, T.; Horiata, M.; Kondo, M.; Itoh, K. *Organometallics* **1989**, *8*, 846–848. (b) Nishiyama, H.; Kondo, M.; Nakamura, T.; Itoh, K. *Organometallics* **1991**, *10*, 500–508.

(10) (a) Carmona, D.; Viguri, F.; Lahoz, F. J.; Oro, L. A. *Inorg. Chem.* **2002**, *41*, 2385–2388, and references therein. (b) Higgins, S. J.; La Pensée, A.; Stuart, C. A.; Charnock, J. M. *J. Chem. Soc., Dalton Trans.* **2001**, 902–910. (c) Albano, V. G.; Di Serio, M.; Monari, M.; Orabona, I.; Panunzi, A.; Ruffo, F. *Inorg. Chem.* **2002**, *41*, 2672–2677. (d) Zhang, K.; Prabhavathy, J.; Yip, J. H. K.; Koh, L. L.; Tan, G. K.; Vittal, J. J. *J. Am. Chem. Soc.* **2003**, *125*, 8452–8453.

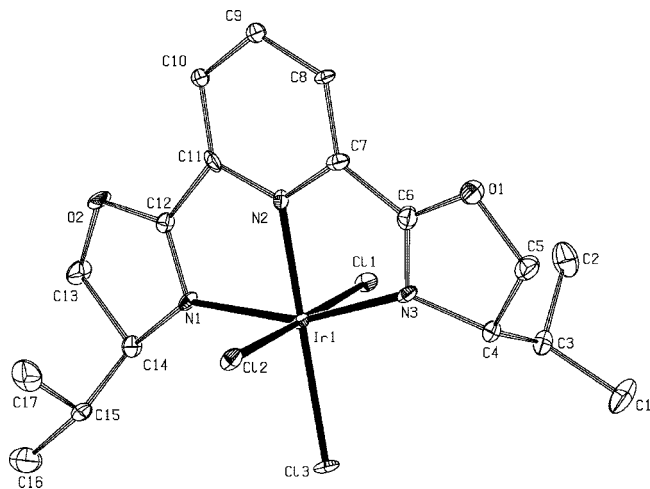


**Figure 4.** ORTEP-type view of the unit  $[\text{IrCl}_3\{\kappa^3\text{-}N,N,N\text{-(}S,S\text{)-}^i\text{Pr-pybox}\}]$  of the complex  $[\text{IrCl}_2\{\kappa^3\text{-}N,N,N\text{-(}S,S\text{)-}^i\text{Pr-pybox}\}(\mu\text{-Cl})\text{Tl}][\text{PF}_6]\cdot\text{Me}_2\text{CO}$  (**14c**· $\text{Me}_2\text{CO}$ ) showing atom-labeling scheme. Thermal ellipsoids are drawn at 20% probability. Hydrogen atoms have been omitted for clarity.

the uncoordinated  $\text{BF}_4^-$  anion ( $1050\text{--}1063\text{ cm}^{-1}$ ), and the elemental analyses of the products are consistent with the stoichiometry  $[\text{IrCl}_3(\kappa^3\text{-}N,N,N\text{-R-pybox})]\cdot\text{AgBF}_4$ . In addition, an electrospray MS analysis performed for complexes **14a** and **15a** clearly evidences the presence of species containing Ir and Ag. Thus, the most significant electrospray MS peaks of **14a** appear at  $m/z = 708$  (43%), 1307 (100%) with the isotopic distribution expected for the  $[\text{IrCl}_3(^i\text{Pr-pybox})\text{Ag}]^+$  and  $[\{\text{IrCl}_3(^i\text{Pr-pybox})\}_2\text{Ag}]^+$  fragments, respectively. In the case of complex **15a** the peak at  $m/z = 776$  (100%,  $[\text{IrCl}_3(\text{Ph-pybox})\text{Ag}]^+$  is observed. All these data suggest a cationic structure with the Ir and Ag atoms likely linked via a chlorine bridge. On the basis of these results, the structure  $[\text{IrCl}_2(\kappa^3\text{-}N,N,N\text{-R-pybox})(\mu\text{-Cl})\text{Ag}][\text{BF}_4]$  is tentatively assigned for complexes **14a** and **15a**. The hexafluoroantimonate complexes **14b** and **15b**, prepared in a similar way using the corresponding  $\text{AgSbF}_6$  salt, display comparable NMR spectroscopic data to **14a** and **15a**, respectively, and show accurate elemental analyses for their stoichiometry (see Experimental Section). Unfortunately, attempts to obtain single crystals of complexes **14a,b** and **15a,b** suitable for X-ray structure determination continuously failed. The long period of time required for crystals to grow results in slow  $\text{AgCl}$  precipitation.

On the other hand, the treatment of complexes **12** and **13** with  $\text{TlPF}_6$  at room temperature gives rise exclusively to complexes  $[\text{IrCl}_2(\kappa^3\text{-}N,N,N\text{-R-pybox})(\mu\text{-Cl})\text{Tl}][\text{PF}_6]$  (**14c** and **15c**) (Scheme 6). Significantly, removing the chloride ligand does not take place in spite of the well-known capability of thallium(I) salts for halide abstraction. Complexes **14c** and **15c** have been characterized by elemental analysis, mass spectra (ESI), and IR and NMR spectroscopy (see Experimental Section for details). The electrospray MS analysis achieved for complexes **14c** and **15c** denotes the presence of species containing Ir and Tl. Thus, relevant electrospray MS peaks appear at  $m/z = 804$  (33%,  $[\text{IrCl}_3(^i\text{Pr-pybox})\text{Tl}]^+$ ) (complex **14c**) and at  $m/z = 872$  (100%,  $[\text{IrCl}_3(\text{Ph-pybox})\text{Tl}]^+$ ) (complex **15c**). The molar conductivity values found for complexes **14c** ( $70\text{ }\Omega^{-1}\text{ cm}^2\text{ mol}^{-1}$ ) and **15c** ( $69\text{ }\Omega^{-1}\text{ cm}^2\text{ mol}^{-1}$ ) are lower than those expected for univalent electrolytes ( $100\text{--}140\text{ }\Omega^{-1}\text{ cm}^2$

**Table 2.** Selected Bond Distances (Å) and Angles (deg) for Complex **14c**· $\text{Me}_2\text{CO}$

bond	distance	bond	distance
Ir–N(2)	1.988(9)	Tl–O(3)	2.701(12)
Ir–N(3)	2.036(9)	Tl–Cl(3)	3.083(3)
Ir–N(1)	2.074(8)	Tl–Cl(2)	3.201
Ir–Cl(2)	2.351(3)	Tl–Cl(1)*	3.194
Ir–Cl(1)	2.352(2)	Tl–Cl(3)*	3.405
Ir–Cl(3)	2.385(2)	Tl–F(2)	3.010
angle	value	angle	value
N(3)–Ir–N(1)	158.9(3)	N(1)–Ir–Cl(3)	101.4(3)
N(2)–Ir–N(3)	79.6(3)	N(3)–Ir–Cl(2)	89.4(3)
N(2)–Ir–N(1)	79.3(3)	N(3)–Ir–Cl(1)	92.6(3)
N(2)–Ir–Cl(2)	89.9(3)	N(3)–Ir–Cl(3)	99.6(3)
N(2)–Ir–Cl(3)	178.9(3)	Cl(2)–Ir–Cl(3)	89.29(10)
N(2)–Ir–Cl(1)	89.8(3)	Cl(1)–Ir–Cl(3)	90.97(9)
N(1)–Ir–Cl(2)	92.5(3)	Cl(2)–Ir–Cl(1)	177.95(10)
N(1)–Ir–Cl(1)	85.4(3)		

$\text{mol}^{-1}$ ).<sup>11</sup> These values can be explained by assuming that the  $\text{PF}_6^-$  anion in solution maintains some degree of association with the thallium ion. In fact, interactions between thallium and  $\text{PF}_6^-$  anions can be deduced from the crystal structure of complex **14c**· $\text{Me}_2\text{CO}$  (see below). Slow diffusion of hexane into a saturated solution of **14c** in acetone provided crystals for an X-ray crystal structure analysis. The asymmetric unit consists of one molecule of  $[\text{IrCl}_3\{\kappa^3\text{-}N,N,N\text{-(}S,S\text{)-}^i\text{Pr-pybox}\}]$ , one  $\text{Tl}^+$  cation, one  $\text{PF}_6^-$  anion, and one molecule of acetone (**14c**· $\text{Me}_2\text{CO}$ ). An ORTEP-type representation of the unit  $[\text{IrCl}_3\{\kappa^3\text{-}N,N,N\text{-(}S,S\text{)-}^i\text{Pr-pybox}\}]$  of complex **14c**· $\text{Me}_2\text{CO}$  is shown in Figure 4, and selected bonding data are listed in Table 2. The representation shows the expected distorted octahedral coordination of the iridium atom, which is bonded to the three chlorine atoms and to the three pybox nitrogen atoms (Figure 4). The N(1)–Ir–N(3) bond angle ( $158.9(3)^\circ$ ) in structure **14c**· $\text{Me}_2\text{CO}$  is slightly larger than those found in all other structures described throughout this study ( $155.6(3)^\circ$  (**1**),  $154.0(2)^\circ$  (**8**), and  $155.6(2)^\circ$  (**10**)). The Cl(3) atom is also bonded to the thallium atom, thus acting as a bridging ligand, Ir(1)–Cl(3)–Tl (see Figure 5 and Table 2). The bond length Cl(3)–Tl ( $3.083(3)\text{ Å}$ ) is somewhat shorter than either the interionic distance in  $\text{TlCl}$  ( $3.15$  and  $3.32\text{ Å}$  for the  $\text{NaCl}$  or  $\text{CsCl}$  forms) or the sum of the van der Waals radius of the chlorine atom and the ionic radius of  $\text{Tl}^+$  ( $3.48\text{ Å}$ ). Moreover, such a length is within the average lengths reported for known  $\text{M–Cl–Tl}^+$  complexes.<sup>12</sup> Figure 5 shows the thallium environment in the molecular structure of **14c**· $\text{Me}_2\text{CO}$ . The Tl cation is also bonded to the acetone oxygen atom ( $2.701(12)\text{ Å}$ ). The

(11) Geary, W. J. *Coord. Chem. Rev.* **1971**, 7, 81–122.

(12) (a) To the best of our knowledge, only the following  $\text{M}-(\mu\text{-X})\text{-Tl}$  structural units have been reported. Cr( $\mu\text{-Cl}$ )Tl: Brian Davis, K.; David Harris, T.; Castellani, M. P.; Golen, J. A.; Rheingold, A. L. *Organometallics* **2007**, 26, 4843–4845. Rh( $\mu\text{-Cl}$ )Tl: (b) Ezomo, O. J.; Mings, D. M. P.; Williams, I. D. *J. Chem. Soc., Chem. Commun.* **1987**, 924–925. Cu( $\mu\text{-Cl}$ )Tl: (c) Kahwa, I. A.; Miller, D.; Mitchell, M.; Fronczek, F. R.; Goodrich, R. G.; Williams, D. J.; O'Mahoney, C. A.; Slawin, A. M.; Ley, S. V.; Groombridge, C. J. *Inorg. Chem.* **1992**, 31, 3963–3970. Y( $\mu\text{-Cl}$ )Tl: (d) Kunrath, F. A.; Casagrande, O. L., Jr.; Toupet, L.; Carpentier, J.-F. *Eur. J. Inorg. Chem.* **2004**, 4803–4806. M( $\mu\text{-Cl}$ )Tl (M = Pd, Pt): (e) Devic, T.; Batail, P.; Fourmigué, M.; Avarvari, N. *Inorg. Chem.* **2004**, 43, 3136–3141. Ru( $\mu\text{-Cl}$ )Tl: (f) Blake, A. J.; Christie, R. M.; Roberts, Y. V.; Sullivan, M. J.; Schröder, M.; Yellowlees, L. J. *J. Chem. Soc., Chem. Commun.* **1992**, 848–849. (g) Bianchini, C.; Masi, D.; Linn, K.; Mealli, C.; Peruzzini, M.; Zanobini, F. *Inorg. Chem.* **1992**, 31, 4036–4037. (h) Drouin, S. D.; Foucault, H. M.; Yap, G. P. A.; Fogg, D. E. *Organometallics* **2004**, 23, 2583–2590. (i) Szymczak, N. K.; Han, F.; Tyler, D. R. *Dalton Trans.* **2004**, 3941–3942. Ru( $\mu\text{-F}$ )Tl: (j) Barthazy, P.; Togni, A.; Mezzetti, A. *Organometallics* **2001**, 20, 3472–3477. (k) Becker, C.; Kieltch, I.; Brogini, D.; Mezzetti, A. *Inorg. Chem.* **2003**, 42, 8417–8429.

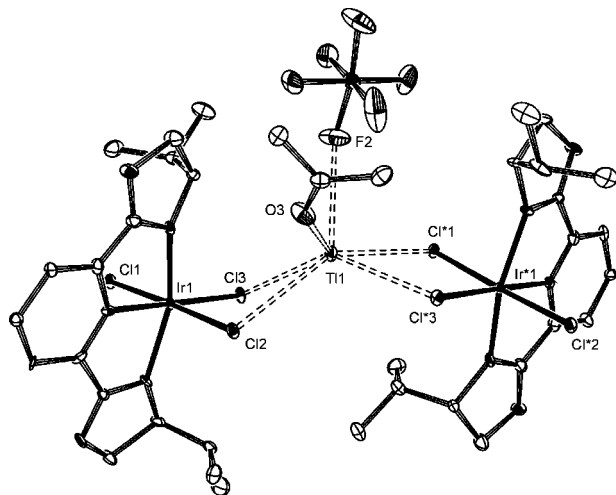


**Figure 5.** ORTEP drawing of the thallium environment in the molecular structure of **14c**·Me<sub>2</sub>CO. Thermal ellipsoids are drawn at 20% probability. Hydrogen atoms have been omitted for clarity.

Tl–O distance is shorter than the sum of the covalent radius of the oxygen atom (Csp<sup>2</sup>=O) and the ionic radius of Tl<sup>+</sup> (2.98 Å). The bond angles O(3)–Tl–Cl(3) and Ir(1)–Cl(3)–Tl are 85.6(3)° and 103.17(9)°, respectively. Further interactions involve the intramolecular Tl–Cl(2) coordination and the intermolecular Tl–Cl(1)\* and Tl–Cl(3)\* coordination, with Tl···Cl distances of 3.201, 3.194, and 3.405 Å, respectively. In addition, the thallium cation is placed close to the PF<sub>6</sub><sup>–</sup> counterion, with a Tl···F(2) distance of 3.010 Å; such a distance is shorter than the sum of the van der Waals radius of the fluorine atom and the ionic radius of the thallium cation (3.25 Å). Each of the Cl(3) atoms is also interacting with a second thallium atom, giving rise to a three-dimensional structure. It is noteworthy that only a few examples of complexes containing the [M–X–Tl] (M = transition metal, X = F, Cl) unit are known,<sup>12</sup> and also that, to the best of our knowledge, the first structure containing the Ir–X–Tl (X = halide) linkage is herein reported.

**Catalytic Transfer Hydrogenation of Ketones.** Recently we reported the first example of asymmetric transfer hydrogenation of ketones with chiral pybox complexes.<sup>5b</sup> Thus, *cis*- and *trans*-[RuCl<sub>2</sub>(L){κ<sup>3</sup>-*N,N,N*-(*R,R*)-Ph-pybox}] (L = phosphine or phosphite) complexes were found to be active catalysts for the formation of *sec*-alcohols with a high level of conversion and enantioselectivity. Indeed, some of them behave as efficient as the best catalysts previously reported (up to 94% ee). The oxazoline phenyl and isopropyl substituents have been shown to be crucial in the case of ruthenium catalysts, the highest ee values being obtained with phenyl-substituted pybox ligands.<sup>5b</sup> These results encouraged us to explore the catalytic activity of some of the iridium complexes herein reported. For comparative purposes we first studied the catalytic activity of both (*S,S*)-<sup>i</sup>Pr-pybox and (*R,R*)-Ph-pybox iridium complexes. Table 3 summarizes the conversion of acetophenone into 1-phenylethanol using the catalysts (*S,S*)-<sup>i</sup>Pr-pybox (**1**, **4**, **12**) and (*R,R*)-Ph-pybox (**3**, **5**, **13**). In a typical experiment the iridium catalyst precursor (0.2 mol %) was added to a solution of ketone in <sup>i</sup>PrOH and stirred for 15 min at 82 °C. Then NaOH was added and the reaction monitored by gas chromatography. Although both (*S,S*)-<sup>i</sup>Pr-pybox and (*R,R*)-Ph-pybox iridium complexes are active catalysts, we observed that the <sup>i</sup>Pr-pybox iridium derivatives show better efficiency and enantioselectivity (see entries

**Table 3.** Catalytic Activity of (*S,S*)-<sup>i</sup>Pr-pybox- and (*R,R*)-Ph-pybox-Containing Iridium Complexes for Transfer Hydrogenation of Acetophenone<sup>a</sup>

	catalyst	<i>t</i> (h)	conv (%)	ee (%) <sup>b</sup>
1	[Ir(η <sup>2</sup> -C <sub>2</sub> H <sub>4</sub> ) <sub>2</sub> ( <sup>i</sup> Pr-pybox)][PF <sub>6</sub> ] ( <b>1</b> )	2(6)	66(95)	50(45) ( <i>R</i> )
2	[IrClH(η <sup>2</sup> -C <sub>2</sub> H <sub>4</sub> )( <sup>i</sup> Pr-pybox)][PF <sub>6</sub> ] ( <b>4</b> )	2	96	67 ( <i>R</i> )
3	[IrCl <sub>3</sub> ( <sup>i</sup> Pr-pybox)] ( <b>12</b> )	2	95	56 ( <i>R</i> )
4	[Ir(η <sup>2</sup> -C <sub>2</sub> H <sub>4</sub> ) <sub>2</sub> (Ph-pybox)][PF <sub>6</sub> ] ( <b>3</b> )	3	83	6 ( <i>S</i> )
5	[IrClH(η <sup>2</sup> -C <sub>2</sub> H <sub>4</sub> )(Ph-pybox)][PF <sub>6</sub> ] ( <b>5</b> )	3	91	20 ( <i>S</i> )
6 <sup>c</sup>	[IrCl <sub>3</sub> (Ph-pybox)] ( <b>13</b> )	3(7)	70(96)	13(15) ( <i>S</i> )

<sup>a</sup> Reactions were carried out at 82 °C using 0.1 M acetophenone solution in 50 mL of 2-propanol using 0.2 mol % catalyst and NaOH (ketone/catalyst/NaOH, 500:1:24). <sup>b</sup> Determined by GC with a Supelco β-DEX 120 chiral capillary column. Absolute configuration determined by comparing optical rotations with literature values. <sup>c</sup> Reaction carried out using KOH (ketone/catalyst/KOH, 500:1:48).

1–3 vs 4–6).<sup>13</sup> The secondary alcohols having the *R* configuration were formed using <sup>i</sup>Pr-pybox catalysts.

The efficiency and asymmetric induction of the catalyst seem to depend on the remaining ligands and probably on the oxidation state of iridium. Thus, the <sup>i</sup>Pr-pybox iridium(I) complex **1** (entry 1) gives rise to rather lower conversion and enantioselectivity than the corresponding iridium(III) complexes **4** and **12** (entries 2 and 3). However, a few iridium(III) complexes have been described for asymmetric transfer hydrogenation of ketones,<sup>14</sup> and no comparative studies on the activity of Ir(I) and Ir(III) have been reported.

We next evaluated the efficiency of several <sup>i</sup>Pr-pybox iridium(III) derivatives and compared with that of the [Ir(μ-Cl)(η<sup>2</sup>-C<sub>8</sub>H<sub>14</sub>)<sub>2</sub>]<sub>2</sub>/<sup>i</sup>Pr-pybox mixture and of the iridium(I) complexes [Ir(η<sup>2</sup>-C<sub>2</sub>H<sub>4</sub>)<sub>2</sub>(<sup>i</sup>Pr-pybox)][Y] [Y = PF<sub>6</sub>, SbF<sub>6</sub>]. We have selected iridium(III) complexes wherein a vacant site, easily available by ligand dissociation or halogen extraction, would allow for ketone coordination as well as hydride complexes on the assumption that hydride complexes are the active species in the transfer hydrogenation process (see Table 4). However, iridium hydride complexes have been sparingly explored in this type of processes, to the best of our knowledge.<sup>14a,15</sup>

We have observed that the iridium(III) complexes are superior in terms of enantioselectivity to the [Ir(μ-Cl)(η<sup>2</sup>-C<sub>8</sub>H<sub>14</sub>)<sub>2</sub>]<sub>2</sub>/<sup>i</sup>Pr-pybox mixture (entries 5, 6, 7, 10, 11 vs entry 1), while the efficiency of the latter appears to be rather better than that of the bisethylene-iridium(I) complexes (entry 1 vs entries 2, 3). The effect of the counterion is of great importance, the asymmetric induction being much lower in the case of hexafluoroantimonate salts (compare entries 3, 12 vs 2, 11, respectively).

The results obtained with hydride catalysts are outlined in entries 4–7. First, no conversion was observed with the hydride complex **4** under base-free conditions (entry 4), due probably to its instability in solution, while conducting the reaction in the presence of NaOH allowed 96% conversion and 67% ee to be achieved (entry 5). Complexes [IrClH(CO)(<sup>i</sup>Pr-pybox)][PF<sub>6</sub>]

(13) This finding is in clear contrast with the results obtained with ruthenium–pybox complexes: see ref 5b.

(14) (a) Murata, K.; Ikariya, T.; Noyori, R. *J. Org. Chem.* **1999**, *64*, 2186–2187. (b) Thorpe, T.; Blacker, J.; Brown, S. M.; Bubert, C.; Crosby, J.; Fitzjohn, S.; Muxworthy, J. P.; Williams, J. M. *J. Tetrahedron Lett.* **2001**, *42*, 4041–4043. (c) Furegati, M.; Rippert, A. *J. Tetrahedron: Asymmetry* **2005**, *16*, 3947–3950.

(15) (a) Chen, J.-S.; Li, Y.-Y.; Dong, Z.-R.; Li, B.-Z.; Gao, J.-X. *Tetrahedron Lett.* **2004**, *45*, 8415–8418. (b) Dong, Z.-R.; Li, Y.-Y.; Chen, J.-S.; Li, B.-Z.; Xing, Y.; Gao, J.-X. *Org. Lett.* **2005**, *7*, 1043–1045. (c) Chen, G.; Xing, Y.; Zhang, H.; Gao, J.-X. *J. Mol. Catal. A: Chem.* **2007**, *273*, 284–288.



**Table 4. Transfer Hydrogenation of Acetophenone Catalyzed by <sup>i</sup>Pr-pybox Iridium(I) and Iridium(III) Complexes<sup>d</sup>**

	catalyst	t (h)	conv (%)	ee (%) (R)
1	[Ir( $\mu$ -Cl)( $\eta^2$ -C <sub>8</sub> H <sub>14</sub> ) <sub>2</sub> ] <sub>2</sub> + <sup>i</sup> Pr-pybox	3	95	51
2	[Ir( $\eta^2$ -C <sub>2</sub> H <sub>4</sub> ) <sub>2</sub> ( <sup>i</sup> Pr-pybox)][PF <sub>6</sub> ] ( <b>1</b> )	2(6)	66(95)	50(45)
3	[Ir( $\eta^2$ -C <sub>2</sub> H <sub>4</sub> ) <sub>2</sub> ( <sup>i</sup> Pr-pybox)][SbF <sub>6</sub> ] ( <b>2</b> )	2	97	10
4 <sup>a</sup>	[IrClH( $\eta^2$ -C <sub>2</sub> H <sub>4</sub> )( <sup>i</sup> Pr-pybox)][PF <sub>6</sub> ] ( <b>4</b> )	2		
5	[IrClH( $\eta^2$ -C <sub>2</sub> H <sub>4</sub> )( <sup>i</sup> Pr-pybox)][PF <sub>6</sub> ] ( <b>4</b> )	2	96	67
6	[IrClH(CO)( <sup>i</sup> Pr-pybox)][PF <sub>6</sub> ] <sup>2b</sup>	3	89	57
7	[IrClH(MeCN)( <sup>i</sup> Pr-pybox)][PF <sub>6</sub> ] ( <b>6</b> )	2	98	55
8	[IrI <sub>2</sub> ( $\eta^2$ -C <sub>2</sub> H <sub>4</sub> )( <sup>i</sup> Pr-pybox)][PF <sub>6</sub> ] ( <b>8</b> )	5	96	54
9	[IrCl( $\eta^3$ -C <sub>3</sub> H <sub>5</sub> )( <sup>i</sup> Pr-pybox)][PF <sub>6</sub> ] ( <b>10</b> )	1.5	97	36
10	[IrCl <sub>3</sub> ( <sup>i</sup> Pr-pybox)] ( <b>12</b> )	2	95	56
11 <sup>b</sup>	[IrCl <sub>2</sub> ( <sup>i</sup> Pr-pybox)( $\eta$ -Cl)Ag][BF <sub>4</sub> ] ( <b>14a</b> )	1.5	96	65
12 <sup>b</sup>	[IrCl <sub>2</sub> ( <sup>i</sup> Pr-pybox)( $\eta$ -Cl)Ag][SbF <sub>6</sub> ] ( <b>14b</b> )	1.5	99	25
13 <sup>c</sup>	[IrCl <sub>2</sub> ( <sup>i</sup> Pr-pybox)( $\eta$ -Cl)Ti][PF <sub>6</sub> ] ( <b>14c</b> )	1	95	65

<sup>a</sup> Reaction carried out under base-free conditions. <sup>b</sup> Reaction carried out using KOH (catalyst/KOH, 1:24). <sup>c</sup> Reaction carried out using KOH (catalyst/KOH, 1:48). <sup>d</sup> Reactions were carried out at 82 °C using 0.1 M acetophenone solution in 50 mL of 2-propanol using 0.2 mol % catalyst and NaOH (ketone/catalyst/NaOH, 500:1:24).

(entry 6) and **6** (entry 7) catalyze the reduction of acetophenone with lower efficiency than complex **4**. In terms of the auxiliary ligand, the enantioselectivity increases on going from CO or MeCN (entries 6, 7) to ethylene (entry 5).

Therefore, we next examined the optimization of the reaction conditions for complexes **4**, **6**, **12**, and **14a**. The following parameters have been explored: (i) The concentration: the best results were obtained with 0.1 M concentration of acetophenone. A more concentrated solution (0.2 M) resulted in slightly lower enantioselectivity. (ii) The base: KOH has been found to be the base of choice among other bases tested (NaOH, CsOH, KO<sup>t</sup>Bu). Furthermore, the best KOH/catalyst ratio was found to be 48:1. (iii) Experimental: It was observed that the addition sequence of reagents as well as the heating time before treatment with the base influences the process. The best results are obtained by addition of the iridium catalyst precursor to a solution of ketone in <sup>i</sup>PrOH, stirring of the resulting mixture at 82 °C for 15 min, and finally addition of KOH.

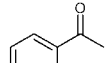
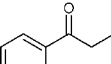
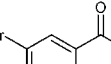
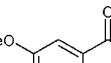
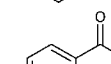
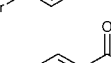
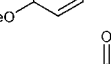
On the basis of these results, the following reaction conditions were chosen: 0.1 M ketone, 0.2 mol % catalyst, T = 82 °C, KOH/catalyst ratio = 48:1, and 50 mL of 2-propanol. The results of the reduction of various aryl ketones to the corresponding secondary alcohols with the precatalyst complex **12**, under optimized reaction conditions, are shown in Table 5.

With the exception of *p*-bromoacetophenone and *p*-methoxyacetophenone, all reactions went to completion in 1 h (97–99% yield). On the other hand, the hydrogenation reaction of *ortho*- and, particularly, *para*-bromoacetophenone results in notable decreasing of the enantioselectivity (entry 1 vs entries 3, 5).

Finally, the selected precatalyst complexes **4**, **6**, **12**, and **14a** were screened in the catalytic reduction of acetophenone, propiophenone, and 4'-methoxyacetophenone (Table 6). Although, no notable differences were found in terms of enantioselectivity and conversion, complex **14a** can be regarded as the catalyst of choice, as it continuously provides higher asymmetric induction.

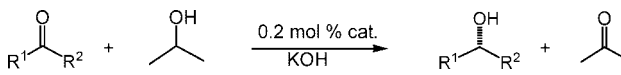
**Concluding Remarks.** In summary we have accomplished the synthesis of enantiopure Ir(I) complexes of the type [Ir( $\eta^2$ -C<sub>2</sub>H<sub>4</sub>)<sub>2</sub>( $\kappa^3$ -*N,N,N*-R-pybox)][Y] and their transformation into Ir(III) complexes by stereoselective oxidative addition. Specifically, the synthesis of hydride–olefin and allyl derivatives is noteworthy. Importantly, Ir(III) complexes of the type [IrCl<sub>3</sub>( $\kappa^3$ -*N,N,N*-R-pybox)] are directly synthesized by addition of chlorine to a mixture of [Ir( $\mu$ -Cl)( $\eta^2$ -C<sub>8</sub>H<sub>14</sub>)<sub>2</sub>]<sub>2</sub> and pybox with high yield.

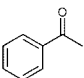
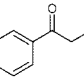
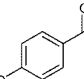
**Table 5. Transfer Hydrogenation of Ketones Catalyzed by Complex [IrCl<sub>3</sub>(<sup>i</sup>Pr-pybox)] (**12**) under Optimized Conditions<sup>a</sup>**

$R^1-C(=O)-R^2 + \text{CH}_3-CH(OH)-CH_3 \xrightarrow[\text{KOH}]{0.2 \text{ mol \% cat.}}$		$R^1-CH(OH)-R^2 + \text{CH}_3-C(=O)-CH_3$		
	Ketone	t (h)	Conv. (%)	e.e. (%) (R)
1		1	97	65
2		1	97	68
3		1	99	43
4		1	98	59
5		1.5	85	19
6		1	85	68
7		1	97	60

<sup>a</sup> Reactions were carried out at 82 °C using 0.1 M ketone solution in 50 mL of 2-propanol, 0.2 mol % catalyst, and KOH (ketone/catalyst/KOH, 500:1:48).

**Table 6. Transfer Hydrogenation of Ketones Catalyzed by Selected <sup>i</sup>Pr-pybox Iridium(III) Complexes under Optimized Conditions<sup>a</sup>**



	Ketone	Catalyst	t (h)	Conv. (%)	e.e. (%) ( <i>R</i> )
1		<b>4</b>	1	96	66
2		<b>6</b>	1.5	97	55
3		<b>12</b>	1	97	65
4		<b>14a</b>	0.75	95	70
5		<b>4</b>	2	97	77
6		<b>6</b>	1.5	97	57
7		<b>12</b>	1	97	68
8		<b>14a</b>	1.5	91	77
9		<b>4</b>	1.5	83	69
10		<b>6</b>	3	84	54
11		<b>12</b>	1	85	68
12		<b>14a</b>	2	83	73

<sup>a</sup> Reactions were carried out at 82 °C using 0.1 M ketone solution in 50 mL of 2-propanol, 0.2 mol % catalyst, and KOH (ketone/catalyst/KOH, 500:1:48).

These chloro-containing Ir(III) complexes are excellent precursors for uncommon heterobimetallic complexes in which both metals are bridged by the chlorine ligand. In this context, the X-ray crystal structure of [IrCl<sub>2</sub>{ $\kappa^3$ -*N,N,N*-(*S,S*)-<sup>i</sup>Pr-pybox}( $\mu$ -Cl)Ti][PF<sub>6</sub>], the first complex containing the Ir–X–Ti<sup>I</sup> linkage, is reported. Preliminary studies on the asymmetric transfer

hydrogenation of ketones reveal the complexes **4**, **6**, **12**, and **14a** to show promising catalytic activity.

## Experimental Section

**General Procedures.** The reactions were performed under an atmosphere of dry nitrogen using vacuum-line and standard Schlenk techniques. All reagents were obtained from commercial suppliers and used without further purification. Solvents were dried by standard methods and distilled under nitrogen before use. The complexes  $[\text{Ir}(\mu\text{-Cl})(\eta^2\text{-C}_8\text{H}_{14})_2]_2$  ( $\text{C}_8\text{H}_{14}$  = cyclooctene),  $[\text{IrClH}(\text{CO})\{\kappa^3\text{-N,N,N,N-(S,S)-'Pr-pybox}\}][\text{PF}_6]$ , and  $[\text{Ir}(\eta^2\text{-C}_2\text{H}_4)_2\{\kappa^3\text{-N,N,N,N-(R,R)-Ph-pybox}\}][\text{PF}_6]$  (**3**) were prepared by previously reported methods.<sup>2b,16</sup> Infrared spectra were recorded on a Perkin-Elmer FT Paragon 1000 spectrometer. The conductivities were measured at room temperature, in ca.  $5 \times 10^{-4}$  mol L<sup>-1</sup> acetone solutions, with a Jenway PCM3 conductimeter. The C, H, and N analyses were carried out with a Perkin-Elmer 240-B microanalyzer. Mass spectra (FAB) were determined with a VG-AUTOSPEC mass spectrometer, operating in the positive mode; 3-nitrobenzyl alcohol (NBA) was used as the matrix. Mass spectra (MALDI-TOF) were determined with a Microflex Bruker spectrometer, operating in the positive mode; dihydroxyanthranol was used as the matrix. Electrospray mass spectra (ESI-MS) were recorded on a Bruker MicroTof-Q instrument, operating in the positive mode and using methanol solutions. NMR spectra were recorded on a Bruker AC300 (DPX-300 or AV-300) instrument at 300 MHz (<sup>1</sup>H) or 75.4 MHz (<sup>13</sup>C) or a Bruker AMX-400 instrument at 400 MHz (<sup>1</sup>H) or 100.6 MHz (<sup>13</sup>C), using SiMe<sub>4</sub> as standard. DEPT experiments were carried out for all the complexes reported. Coupling constants (*J*) are given in hertz. Abbreviations used: s, singlet; d, doublet; dd, doublet of doublets; t, triplet; pt, pseudotriplet; m, multiplet; q, quartet; br, broad.

**Synthesis of Complexes  $[\text{Ir}(\eta^2\text{-C}_2\text{H}_4)_2\{\kappa^3\text{-N,N,N,N-(S,S)-'Pr-pybox}\}][\text{Y}]$  (*Y* = PF<sub>6</sub> (**1**), SbF<sub>6</sub> (**2**)).** A slow flow of ethylene was bubbled into a suspension of  $[\text{Ir}(\mu\text{-Cl})(\eta^2\text{-C}_8\text{H}_{14})_2]_2$  (0.448 g, 0.5 mmol) in 5 mL of methanol at room temperature. Once the color of the mixture changed to yellow, 'Pr-pybox (0.301 g, 1 mmol) was added and stirred at -40 °C for 40 min. The formation of a red solution was observed. NaY (*Y* = PF<sub>6</sub>, SbF<sub>6</sub>) (1.45 mmol) was added, and the mixture was stirred at -40 °C for 45 min. Diethyl ether was added (ca. 100 mL), and the resulting solid was filtered, washed with cold diethyl ether (3 × 5 mL), and then vacuum-dried.

**Complex 1.** Yield: 94% (0.653 g). Color: orange. IR (KBr, ν, cm<sup>-1</sup>): 842 (PF<sub>6</sub><sup>-</sup>). Molar conductivity (acetone 20 °C, Ω<sup>-1</sup> cm<sup>2</sup> mol<sup>-1</sup>): 137. <sup>1</sup>H NMR (300 MHz, acetone-*d*<sub>6</sub>, 293 K): δ 8.33 (m, 3H, C<sub>5</sub>H<sub>3</sub>N), 5.05 (m, 2H, OCH<sub>2</sub>), 4.88 (m, 2H, OCH<sub>2</sub>), 3.86 (m, 2H, CH<sup>i</sup>Pr), 2.89 (br s, 8H, C<sub>2</sub>H<sub>4</sub>), 1.75 (m, 2H, CHMe<sub>2</sub>), 0.95 (d, *J*<sub>HH</sub> = 7.0 Hz, 6H, CHMe<sub>2</sub>), 0.71 (d, 6H, *J*<sub>HH</sub> = 7.0 Hz, CHMe<sub>2</sub>) ppm. <sup>13</sup>C{<sup>1</sup>H} NMR (75.4 MHz, acetone-*d*<sub>6</sub>, 293 K): δ 171.2 (s, OCN), 146.7 (s, C<sup>2,6</sup> C<sub>5</sub>H<sub>3</sub>N), 138.6 (s, C<sup>4</sup>H C<sub>5</sub>H<sub>3</sub>N), 126.9 (s, C<sup>3,5</sup>H C<sub>5</sub>H<sub>3</sub>N), 72.8 (s, OCH<sub>2</sub>), 68.3 (s, CH<sup>i</sup>Pr), 32.1 (s, C<sub>2</sub>H<sub>4</sub>), 30.1 (s, CHMe<sub>2</sub>), 19.4 (s, CHMe<sub>2</sub>), 14.8 (s, CHMe<sub>2</sub>) ppm. <sup>1</sup>H NMR (400 MHz, acetone-*d*<sub>6</sub>, 203 K): δ 8.40 (s, 3H, C<sub>5</sub>H<sub>3</sub>N), 4.96 (m, 4H, OCH<sub>2</sub>), 3.83 (m, 2H, CH<sup>i</sup>Pr), 3.80, 3.50, 2.04, 1.89 (4 × m, 2H each one, C<sub>2</sub>H<sub>4</sub>), 1.64 (m, 2H, CHMe<sub>2</sub>), 0.87 (d, *J*<sub>HH</sub> = 6.6 Hz, 6H, CHMe<sub>2</sub>), 0.65 (d, *J*<sub>HH</sub> = 6.6 Hz, 6H, CHMe<sub>2</sub>) ppm. <sup>13</sup>C{<sup>1</sup>H} NMR (100.6 MHz, acetone-*d*<sub>6</sub>, 203 K): δ 170.2 (s, OCN), 146.2 (s, C<sup>2,6</sup> C<sub>5</sub>H<sub>3</sub>N), 138.1 (s, C<sup>4</sup>H C<sub>5</sub>H<sub>3</sub>N), 126.0 (s, C<sup>3,5</sup>H C<sub>5</sub>H<sub>3</sub>N), 71.8 (s, OCH<sub>2</sub>), 67.1 (s, CH<sup>i</sup>Pr), 36.7 (s, C<sub>2</sub>H<sub>4</sub>), 29.4 (s, CHMe<sub>2</sub>), 23.8 (s, C<sub>2</sub>H<sub>4</sub>), 18.6 (s, CHMe<sub>2</sub>), 13.9 (s, CHMe<sub>2</sub>) ppm. Anal. Calcd for C<sub>21</sub>H<sub>31</sub>N<sub>3</sub>F<sub>6</sub>IrO<sub>2</sub>P (694.67): C 36.31, H 4.50, N 6.05. Found: C 35.98, H 4.24, N 5.81.

**Complex 2.** Yield: 95% (0.746 g). Color: orange. IR (KBr, ν, cm<sup>-1</sup>): 656 (SbF<sub>6</sub><sup>-</sup>). Molar conductivity (acetone 20 °C, Ω<sup>-1</sup> cm<sup>2</sup>

mol<sup>-1</sup>): 142. <sup>1</sup>H NMR (300 MHz, acetone-*d*<sub>6</sub>, 293 K): δ 8.30 (m, 3H, C<sub>5</sub>H<sub>3</sub>N), 5.00 (m, 2H, OCH<sub>2</sub>), 4.88 (m, 2H, OCH<sub>2</sub>), 3.80 (m, 2H, CH<sup>i</sup>Pr), 2.89 (br s, 8H, C<sub>2</sub>H<sub>4</sub>), 1.76 (m, 2H, CHMe<sub>2</sub>), 0.95 (d, *J*<sub>HH</sub> = 7.1 Hz, 6H, CHMe<sub>2</sub>), 0.73 (d, 6H, *J*<sub>HH</sub> = 7.1 Hz, CHMe<sub>2</sub>) ppm. <sup>13</sup>C{<sup>1</sup>H} NMR (75.4 MHz, acetone-*d*<sub>6</sub>, 293 K): δ 171.8 (s, OCN), 146.9 (s, C<sup>2,6</sup> C<sub>5</sub>H<sub>3</sub>N), 138.6 (s, C<sup>4</sup>H C<sub>5</sub>H<sub>3</sub>N), 127.2 (s, C<sup>3,5</sup>H C<sub>5</sub>H<sub>3</sub>N), 73.0 (s, OCH<sub>2</sub>), 68.4 (s, CH<sup>i</sup>Pr), 32.4 (s, C<sub>2</sub>H<sub>4</sub>), 30.2 (s, CHMe<sub>2</sub>), 19.7 (s, CHMe<sub>2</sub>), 14.7 (s, CHMe<sub>2</sub>) ppm. Anal. Calcd for C<sub>21</sub>H<sub>31</sub>N<sub>3</sub>SbF<sub>6</sub>IrO<sub>2</sub> (785.46): C 32.11, H 3.98, N 5.35. Found: C 32.30, H 4.10, N 5.40.

**Synthesis of Complexes  $[\text{IrClH}(\eta^2\text{-C}_2\text{H}_4)(\kappa^3\text{-N,N,N,R-pybox})][\text{PF}_6]$  (*R* = 'Pr (**4**), Ph (**5**)).** A solution of HCl in diethyl ether (1 M, 0.1 mL, 0.1 mmol) was added to a solution of the complex  $[\text{Ir}(\eta^2\text{-C}_2\text{H}_4)_2(\kappa^3\text{-N,N,N,R-pybox})][\text{PF}_6]$  (*R* = 'Pr, Ph) (0.1 mmol) in 5 mL of THF at 0 °C. Immediately the reaction mixture became yellow, and stirring was continued for 5 min. Hexane was added, and the resulting solid was filtered, washed with hexane (2 × 5 mL), and then vacuum-dried.

**Complex 4.** Yield: 94% (0.066 g). Color: yellow. IR (KBr, ν, cm<sup>-1</sup>): 2186 (IrH), 843 (PF<sub>6</sub><sup>-</sup>). Molar conductivity (acetone 20 °C, Ω<sup>-1</sup> cm<sup>2</sup> mol<sup>-1</sup>): 128. <sup>1</sup>H NMR (300 MHz, acetone-*d*<sub>6</sub>, 293 K): δ 8.68 (t, *J*<sub>HH</sub> = 8.1 Hz, 1H, H<sup>4</sup> C<sub>5</sub>H<sub>3</sub>N), 8.44 (d, *J*<sub>HH</sub> = 8.1 Hz, 1H, H<sup>3,5</sup> C<sub>5</sub>H<sub>3</sub>N), 8.43 (d, *J*<sub>HH</sub> = 8.1 Hz, 1H, H<sup>3,5</sup> C<sub>5</sub>H<sub>3</sub>N), 5.20 (m, 4H, OCH<sub>2</sub>), 4.77 (m, 4H, C<sub>2</sub>H<sub>4</sub>), 4.52 (m, 2H, CH<sup>i</sup>Pr), 2.04 (m, 1H, CHMe<sub>2</sub>), 1.87 (m, 1H, CHMe<sub>2</sub>), 1.03 (d, *J*<sub>HH</sub> = 7.2 Hz, 3H, CHMe<sub>2</sub>), 1.02 (d, *J*<sub>HH</sub> = 7.2 Hz, 3H, CHMe<sub>2</sub>), 0.94 (d, *J*<sub>HH</sub> = 6.8 Hz, 3H, CHMe<sub>2</sub>), 0.79 (d, *J*<sub>HH</sub> = 6.8 Hz, 3H, CHMe<sub>2</sub>), -22.56 (s, 1H, IrH) ppm. <sup>13</sup>C{<sup>1</sup>H} NMR (100.6 MHz, acetone-*d*<sub>6</sub>, 233 K): δ 170.7 (s, OCN), 170.4 (s, OCN), 144.4 (s, C<sup>2,6</sup> C<sub>5</sub>H<sub>3</sub>N), 143.5 (s, C<sup>4</sup>H C<sub>5</sub>H<sub>3</sub>N), 128.2 (s, C<sup>3,5</sup>H C<sub>5</sub>H<sub>3</sub>N), 127.8 (s, C<sup>3,5</sup>H C<sub>5</sub>H<sub>3</sub>N), 73.3 (s, OCH<sub>2</sub>), 72.9 (s, OCH<sub>2</sub>), 69.6 (s, CH<sup>i</sup>Pr), 68.0 (s, CH<sup>i</sup>Pr), 60.0 (s, C<sub>2</sub>H<sub>4</sub>), 29.6 (s, CHMe<sub>2</sub>), 29.3 (s, CHMe<sub>2</sub>), 18.1 (s, CHMe<sub>2</sub>), 17.5 (s, CHMe<sub>2</sub>), 14.2 (s, CHMe<sub>2</sub>), 12.7 (s, CHMe<sub>2</sub>) ppm. Anal. Calcd for C<sub>19</sub>H<sub>28</sub>N<sub>3</sub>ClF<sub>6</sub>IrO<sub>2</sub>P (703.08): C 32.46, H 4.01, N 5.98. Found: C 32.26, H 3.94, N 5.83.

**Complex 5.** Yield: 88% (0.068 g). Color: yellow. IR (KBr, ν, cm<sup>-1</sup>): 2173 (IrH), 843 (PF<sub>6</sub><sup>-</sup>). Molar conductivity (acetone 20 °C, Ω<sup>-1</sup> cm<sup>2</sup> mol<sup>-1</sup>): 120. <sup>1</sup>H NMR (300 MHz, acetone-*d*<sub>6</sub>, 293 K): δ 8.79 (m, 1H, H<sup>4</sup> C<sub>5</sub>H<sub>3</sub>N), 8.58 (m, 2H, H<sup>3,5</sup> C<sub>5</sub>H<sub>3</sub>N), 7.46 (m, 10H, Ph), 5.68 (m, 2H, OCH<sub>2</sub>), 5.50 (m, 2H, OCH<sub>2</sub>), 5.03 (m, 1H, CHPh), 4.93 (m, 1H, CHPh), 3.83 (m, 2H, C<sub>2</sub>H<sub>4</sub>), 3.45 (m, 2H, C<sub>2</sub>H<sub>4</sub>), -22.45 (s, 1H, IrH) ppm. <sup>13</sup>C{<sup>1</sup>H} NMR (100.6 MHz, acetone-*d*<sub>6</sub>, 233 K): δ 171.9 (s, OCN), 171.6 (s, OCN), 145.0 (s, C<sup>2,6</sup> C<sub>5</sub>H<sub>3</sub>N), 144.6 (s, C<sup>2,6</sup> C<sub>5</sub>H<sub>3</sub>N), 143.4 (s, C<sup>4</sup>H C<sub>5</sub>H<sub>3</sub>N), 137.9 (s, C<sup>ipso</sup> Ph), 136.9 (s, C<sup>ipso</sup> Ph), 129.4, 129.3, 128.8, 128.3, 127.9 (s, C<sup>3,5</sup>H C<sub>5</sub>H<sub>3</sub>N, Ph), 80.6 (s, OCH<sub>2</sub>), 80.3 (s, OCH<sub>2</sub>), 69.2 (s, CHPh), 67.3 (s, CHPh), 59.5 (s, C<sub>2</sub>H<sub>4</sub>) ppm. Anal. Calcd for C<sub>25</sub>H<sub>24</sub>N<sub>3</sub>ClF<sub>6</sub>IrO<sub>2</sub>P (771.11): C 38.94, H 3.14, N 5.45. Found: C 38.55, H 3.06, N 5.22. FAB-MS: *m/z* 626  $[\text{IrClH}(\text{C}_2\text{H}_4)(\text{Ph-pybox})]^+$ .

**Synthesis of Complexes  $[\text{IrClH}(\text{MeCN})(\kappa^3\text{-N,N,N,R-pybox})][\text{PF}_6]$  (*R* = 'Pr (**6**), Ph (**7**)).** To a solution of complexes  $[\text{IrClH}(\eta^2\text{-C}_2\text{H}_4)(\kappa^3\text{-N,N,N,R-pybox})][\text{PF}_6]$  (*R* = 'Pr (**1**), Ph (**3**)) (0.1 mmol) in acetone (5 mL) was added at 0 °C acetonitrile (1 mL). The reaction mixture was allowed to warm to room temperature and stirred during 30 min. A (1:1) diethyl ether/hexane mixture was added, and the resulting solid was filtered, washed with diethyl ether (3 × 5 mL), and then vacuum-dried.

**Complex 6.** Yield: 84% (0.060 g). Color: orange. IR (KBr, ν, cm<sup>-1</sup>): 2160 (IrH), 842 (PF<sub>6</sub><sup>-</sup>). Molar conductivity (acetone 20 °C, Ω<sup>-1</sup> cm<sup>2</sup> mol<sup>-1</sup>): 132. <sup>1</sup>H NMR (300 MHz, acetone-*d*<sub>6</sub>, 293 K): δ 8.34 (m, 1H, H<sup>4</sup> C<sub>5</sub>H<sub>3</sub>N), 8.18 (m, 2H, H<sup>3,5</sup> C<sub>5</sub>H<sub>3</sub>N), 5.24 (m, 4H, OCH<sub>2</sub>), 4.49 (m, 2H, CH<sup>i</sup>Pr), 3.02 (s, 3H, MeCN), 2.39 (m, 2H, CHMe<sub>2</sub>), 1.08 (m, 9H, CHMe<sub>2</sub>), 0.92 (d, *J*<sub>HH</sub> = 6.8 Hz, 3H, CHMe<sub>2</sub>), -24.79 (s, 1H, IrH) ppm. <sup>13</sup>C{<sup>1</sup>H} NMR (75.4 MHz, acetone-*d*<sub>6</sub>, 293 K): δ 171.9 (s, OCN), 171.8 (s, OCN), 147.7 (2 × s, C<sup>2,6</sup> C<sub>5</sub>H<sub>3</sub>N), 141.2 (s, C<sup>4</sup>H C<sub>5</sub>H<sub>3</sub>N), 127.5 (s, C<sup>3,5</sup>H C<sub>5</sub>H<sub>3</sub>N),



127.4 (s, C<sup>3.5</sup>H C<sub>5</sub>H<sub>3</sub>N), 124.0 (s, MeCN), 74.4 (s, OCH<sub>2</sub>), 74.2 (s, OCH<sub>2</sub>), 71.9 (s, CH<sup>i</sup>Pr), 69.6 (s, CH<sup>i</sup>Pr), 30.7 (s, CHMe<sub>2</sub>), 30.3 (s, CHMe<sub>2</sub>), 19.1 (s, CHMe<sub>2</sub>), 18.5 (s, CHMe<sub>2</sub>), 16.0 (s, CHMe<sub>2</sub>), 14.6 (s, CHMe<sub>2</sub>), 3.6 (s, MeCN) ppm. Anal. Calcd for C<sub>19</sub>H<sub>27</sub>N<sub>4</sub>ClF<sub>6</sub>IrO<sub>2</sub>P (716.08): C 31.87, H 3.80, N 7.82. Found: C 31.80, H 3.76, N 7.98. FAB-MS: *m/z* 571 [IrClH(MeCN)(<sup>i</sup>Pr-pybox)]<sup>+</sup>, 531 [IrClH(<sup>i</sup>Pr-pybox)]<sup>+</sup>.

**Complex 7.** Yield: 86% (0.067 g). Color: orange. IR (KBr,  $\nu$ , cm<sup>-1</sup>): 2165 (IrH), 842 (PF<sub>6</sub><sup>-</sup>). Molar conductivity (acetone 20 °C,  $\Omega^{-1}$  cm<sup>2</sup> mol<sup>-1</sup>): 127. <sup>1</sup>H NMR (400 MHz, CD<sub>2</sub>Cl<sub>2</sub>, 293 K):  $\delta$  8.20 (t,  $J_{\text{HH}} = 8.0$  Hz, 1H, H<sup>4</sup> C<sub>5</sub>H<sub>3</sub>N), 8.06 (m, 2H, H<sup>3.5</sup> C<sub>5</sub>H<sub>3</sub>N), 7.63, 7.47, 7.30 (3  $\times$  m, 10H, Ph), 5.60 (dd,  $J_{\text{HH}} = 9.1$  Hz,  $J_{\text{HH}} = 5.0$  Hz, 1H, OCH<sub>2</sub>), 5.57 (dd,  $J_{\text{HH}} = 9.0$  Hz,  $J_{\text{HH}} = 4.8$  Hz, 1H, OCH<sub>2</sub>), 5.38 (m, 2H, OCH<sub>2</sub>), 4.98 (dd,  $J_{\text{HH}} = 10.5$  Hz,  $J_{\text{HH}} = 9.0$  Hz, 1H, CHPh), 4.86 (dd,  $J_{\text{HH}} = 12.2$  Hz,  $J_{\text{HH}} = 9.1$  Hz, 1H, CHPh), 1.84 (s, 3H, MeCN), -24.93 (s, 1H, IrH) ppm. <sup>13</sup>C{<sup>1</sup>H} NMR (100.6 MHz, acetone-*d*<sub>6</sub>, 293 K):  $\delta$  172.3 (s, OCN), 171.6 (s, OCN), 147.3 (s, C<sup>2.6</sup> C<sub>5</sub>H<sub>3</sub>N), 147.2 (s, C<sup>2.6</sup> C<sub>5</sub>H<sub>3</sub>N), 140.4 (s, C<sup>4</sup>H C<sub>5</sub>H<sub>3</sub>N), 136.9 (s, C<sup>i</sup>iso Ph), 135.8 (s, C<sup>i</sup>iso Ph), 129.5, 129.2, 129.0, 128.9, 128.5, 128.5 (s, Ph), 126.9 (s, C<sup>3.5</sup>H C<sub>5</sub>H<sub>3</sub>N), 126.8 (s, C<sup>3.5</sup>H C<sub>5</sub>H<sub>3</sub>N), 121.0 (s, MeCN), 80.0 (s, OCH<sub>2</sub>), 79.8 (s, OCH<sub>2</sub>), 70.8 (s, CHPh), 68.6 (s, CHPh), 1.8 (s, MeCN) ppm. Anal. Calcd for C<sub>25</sub>H<sub>23</sub>N<sub>4</sub>ClF<sub>6</sub>IrO<sub>2</sub>P (784.11): C 38.29, H 2.96, N 7.15. Found: C 38.05, H 2.88, N 7.30.

**Synthesis of Complexes [IrI<sub>2</sub>( $\eta^2$ -C<sub>2</sub>H<sub>4</sub>)( $\kappa^3$ -*N,N,N*-R-pybox)]-[PF<sub>6</sub>] (R = <sup>i</sup>Pr (8), Ph (9)).** To a solution of [Ir( $\eta^2$ -C<sub>2</sub>H<sub>4</sub>)<sub>2</sub>( $\kappa^3$ -*N,N,N*-R-pybox)][PF<sub>6</sub>] (R = <sup>i</sup>Pr, Ph) (0.2 mmol) in dichloromethane (1 mL) was added I<sub>2</sub> (0.051 g, 0.2 mmol), and the reaction mixture was stirred for 30 min. Diethyl ether was added, and the resulting solid was filtered, washed with diethyl ether (3  $\times$  5 mL), and then vacuum-dried.

**Complex 8.** Yield: 96% (0.177 g). Color: red-brown. IR (KBr,  $\nu$ , cm<sup>-1</sup>): 842 (PF<sub>6</sub><sup>-</sup>). Molar conductivity (acetone 20 °C,  $\Omega^{-1}$  cm<sup>2</sup> mol<sup>-1</sup>): 139. <sup>1</sup>H NMR (300 MHz, acetone-*d*<sub>6</sub>, 293 K):  $\delta$  8.83 (m, 1H, H<sup>4</sup> C<sub>5</sub>H<sub>3</sub>N), 8.72 (m, 2H, H<sup>3.5</sup> C<sub>5</sub>H<sub>3</sub>N), 6.21 (m, 2H, C<sub>2</sub>H<sub>4</sub>), 5.91 (m, 2H, C<sub>2</sub>H<sub>4</sub>), 5.58 (m, 2H, OCH<sub>2</sub>), 5.36 (m, 2H, CH<sup>i</sup>Pr), 4.80 (m, 2H, OCH<sub>2</sub>), 2.53 (m, 2H, CHMe<sub>2</sub>), 1.19 (d,  $J_{\text{HH}} = 7.1$  Hz, 6H, CHMe<sub>2</sub>), 1.04 (d,  $J_{\text{HH}} = 6.6$  Hz, 6H, CHMe<sub>2</sub>) ppm. <sup>13</sup>C{<sup>1</sup>H} NMR (75.4 MHz, acetone-*d*<sub>6</sub>, 293 K):  $\delta$  172.2 (s, OCN), 144.7 (s, C<sup>4</sup>H C<sub>5</sub>H<sub>3</sub>N), 143.9 (s, C<sup>2.6</sup> C<sub>5</sub>H<sub>3</sub>N), 130.9 (s, C<sup>3.5</sup>H C<sub>5</sub>H<sub>3</sub>N), 75.9 (s, OCH<sub>2</sub>), 71.3 (s, C<sub>2</sub>H<sub>4</sub>), 71.3 (s, CH<sup>i</sup>Pr), 30.4 (s, CHMe<sub>2</sub>), 18.8 (s, CHMe<sub>2</sub>), 15.4 (s, CHMe<sub>2</sub>) ppm. Anal. Calcd for C<sub>19</sub>H<sub>27</sub>N<sub>4</sub>F<sub>6</sub>IrO<sub>2</sub>P (920.43): C 24.79, H 2.96, N 4.57; Found: C 24.45, H 2.91, N 4.37. FAB-MS: *m/z* 775 [IrI<sub>2</sub>(C<sub>2</sub>H<sub>4</sub>)(<sup>i</sup>Pr-pybox)]<sup>+</sup>, 747 [IrI<sub>2</sub>(<sup>i</sup>Pr-pybox)]<sup>+</sup>, 620 [IrI(<sup>i</sup>Pr-pybox)]<sup>+</sup>.

**Complex 9.** Yield: 89% (0.175 g). Color: orange. IR (KBr,  $\nu$ , cm<sup>-1</sup>): 844 (PF<sub>6</sub><sup>-</sup>). Molar conductivity (acetone 20 °C,  $\Omega^{-1}$  cm<sup>2</sup> mol<sup>-1</sup>): 132. <sup>1</sup>H NMR (400 MHz, acetone-*d*<sub>6</sub>, 293 K):  $\delta$  8.92 (m, 1H, H<sup>4</sup> C<sub>5</sub>H<sub>3</sub>N), 8.85 (m, 2H, H<sup>3.5</sup> C<sub>5</sub>H<sub>3</sub>N), 7.74, 7.47 (2  $\times$  m, 10H, Ph), 5.86 (m, 4H, C<sub>2</sub>H<sub>4</sub>), 5.34 (m, 2H, OCH<sub>2</sub>), 5.29 (m, 2H, CHPh), 4.94 (m, 2H, OCH<sub>2</sub>) ppm. <sup>13</sup>C{<sup>1</sup>H} NMR (75.4 MHz, acetone-*d*<sub>6</sub>, 293 K):  $\delta$  172.6 (s, OCN), 144.0 (s, C<sup>4</sup>H C<sub>5</sub>H<sub>3</sub>N), 143.6 (s, C<sup>2.6</sup> C<sub>5</sub>H<sub>3</sub>N), 137.0 (s, C<sup>i</sup>iso Ph), 130.9 (s, C<sup>3.5</sup>H C<sub>5</sub>H<sub>3</sub>N), 130.0, 129.5, 129.4 (s, Ph), 81.9 (s, OCH<sub>2</sub>), 70.6 (s, C<sub>2</sub>H<sub>4</sub>), 67.8 (s, CHPh) ppm. Anal. Calcd for C<sub>25</sub>H<sub>23</sub>N<sub>4</sub>F<sub>6</sub>IrO<sub>2</sub>P (988.46): C 30.38, H 2.35, N 4.25. Found: C 30.61, H 2.30, N 4.46.

**Synthesis of Complexes [IrCl( $\eta^3$ -C<sub>3</sub>H<sub>5</sub>)( $\kappa^3$ -*N,N,N*-R-pybox)][PF<sub>6</sub>] (R = <sup>i</sup>Pr (10), Ph (11)).** Allyl chloride (0.026 mL, 0.3 mmol) was added to a solution of the complexes [Ir( $\eta^2$ -C<sub>2</sub>H<sub>4</sub>)<sub>2</sub>( $\kappa^3$ -*N,N,N*-R-pybox)][PF<sub>6</sub>] (R = <sup>i</sup>Pr (1) or Ph (3)) (0.2 mmol) in 10 mL of acetone. The resulting solution was stirred at room temperature for 5 min, and the volatiles were removed under vacuum. The deep red residue was extracted with dichloromethane and filtered. Hexane was added, and the solution was concentrated and cooled to -20 °C, giving a microcrystalline solid, which was washed with hexane (3  $\times$  5 mL) and then vacuum-dried.

**Complex 10.** Yield: 93% (0.133 g). Color: orange. IR (KBr,  $\nu$ , cm<sup>-1</sup>): 843 (PF<sub>6</sub><sup>-</sup>). Molar conductivity (acetone 20 °C,  $\Omega^{-1}$  cm<sup>2</sup> mol<sup>-1</sup>): 135. <sup>1</sup>H NMR (400 MHz, acetone-*d*<sub>6</sub>, 293 K):  $\delta$  8.61 (t,  $J_{\text{HH}} = 8.0$  Hz, 1H, H<sup>4</sup> C<sub>5</sub>H<sub>3</sub>N), 8.48 (dd,  $J_{\text{HH}} = 8.0$  Hz,  $J_{\text{HH}} = 1.0$  Hz, 1H, H<sup>3.5</sup> C<sub>5</sub>H<sub>3</sub>N), 8.39 (dd,  $J_{\text{HH}} = 8.0$  Hz,  $J_{\text{HH}} = 1.0$  Hz, 1H, H<sup>3.5</sup> C<sub>5</sub>H<sub>3</sub>N), 5.60 (m, 1H, CH allyl), 5.29 (m, 1H, OCH<sub>2</sub>), 5.10 (m, 3H, OCH<sub>2</sub>), 4.92 (d,  $J_{\text{HH}} = 6.9$  Hz, 1H, H<sup>syn</sup> allyl), 4.39 (m, 1H, CH<sup>i</sup>Pr), 4.28 (m, 1H, CH<sup>i</sup>Pr), 3.95 (d,  $J_{\text{HH}} = 11.7$  Hz, 1H, H<sup>anti</sup> allyl), 3.52 (d,  $J_{\text{HH}} = 6.9$  Hz, 1H, H<sup>syn</sup> allyl), 2.76 (d,  $J_{\text{HH}} = 11.7$  Hz, 1H, H<sup>anti</sup> allyl), 1.97 (m, 1H, CHMe<sub>2</sub>), 1.63 (m, 1H, CHMe<sub>2</sub>), 1.01 (m, 6H, CHMe<sub>2</sub>), 0.93 (d, 3H,  $J_{\text{HH}} = 6.7$  Hz, CHMe<sub>2</sub>), 0.86 (d, 3H,  $J_{\text{HH}} = 6.7$  Hz, CHMe<sub>2</sub>) ppm. <sup>13</sup>C{<sup>1</sup>H} NMR (75.4 MHz, CD<sub>2</sub>Cl<sub>2</sub>, 293 K):  $\delta$  171.0 (s, OCN), 170.1 (s, OCN), 143.2 (s, C<sup>2.6</sup> C<sub>5</sub>H<sub>3</sub>N), 142.8 (s, C<sup>2.6</sup> C<sub>5</sub>H<sub>3</sub>N), 139.2 (s, C<sup>4</sup>H C<sub>5</sub>H<sub>3</sub>N), 127.0 (s, C<sup>3.5</sup>H C<sub>5</sub>H<sub>3</sub>N), 95.8 (s, CH allyl), 73.0 (s, OCH<sub>2</sub>), 72.1 (s, OCH<sub>2</sub>), 68.7 (s, CH<sup>i</sup>Pr), 67.9 (s, CH<sup>i</sup>Pr), 44.2 (s, CH<sub>2</sub> allyl), 29.1 (s, CHMe<sub>2</sub>), 28.7 (s, CHMe<sub>2</sub>), 27.0 (s, CH<sub>2</sub> allyl), 18.0 (s, CHMe<sub>2</sub>), 17.9 (s, CHMe<sub>2</sub>), 14.6 (s, CHMe<sub>2</sub>), 12.5 (s, CHMe<sub>2</sub>) ppm. Anal. Calcd for C<sub>20</sub>H<sub>28</sub>N<sub>3</sub>ClF<sub>6</sub>IrO<sub>2</sub>P (715.09): C 33.59, H 3.95, N 5.88. Found: C 33.41, H 3.81, N 5.80.

**Complex 11.** Yield: 84% (0.132 g). Color: orange. IR (KBr,  $\nu$ , cm<sup>-1</sup>): 841 (PF<sub>6</sub><sup>-</sup>). Molar conductivity (acetone 20 °C,  $\Omega^{-1}$  cm<sup>2</sup> mol<sup>-1</sup>): 118. <sup>1</sup>H NMR (300 MHz, acetone-*d*<sub>6</sub>, 293 K): major isomer,  $\delta$  8.67 (m, 1H, H<sup>4</sup> C<sub>5</sub>H<sub>3</sub>N), 8.57 (m, 1H, H<sup>3.5</sup> C<sub>5</sub>H<sub>3</sub>N), 8.48 (m, 1H, H<sup>3.5</sup> C<sub>5</sub>H<sub>3</sub>N), 7.52, 7.40 (2  $\times$  m, 10H, Ph), 5.60 (m, 3H, CH allyl, OCH<sub>2</sub>), 5.45 (m, 1H, OCH<sub>2</sub>), 5.22 (m, 1H, OCH<sub>2</sub>), 5.07 (m, 1H, CHPh), 4.87 (m, 1H, CHPh), 4.10 (d,  $J_{\text{HH}} = 4.1$  Hz, 1H, H<sup>syn</sup> allyl), 3.56 (d,  $J_{\text{HH}} = 7.1$  Hz, 1H, H<sup>syn</sup> allyl), 3.25 (m, 1H, H<sup>anti</sup> allyl), 2.24 (d,  $J_{\text{HH}} = 10.0$  Hz, 1H, H<sup>anti</sup> allyl) ppm. <sup>13</sup>C{<sup>1</sup>H} NMR (75.4 MHz, acetone-*d*<sub>6</sub>, 293 K): major isomer,  $\delta$  173.5 (s, OCN), 172.9 (s, OCN), 145.8 (s, C<sup>2.6</sup> C<sub>5</sub>H<sub>3</sub>N), 144.7 (s, C<sup>2.6</sup> C<sub>5</sub>H<sub>3</sub>N), 141.8 (s, C<sup>4</sup>H C<sub>5</sub>H<sub>3</sub>N), 135.8 (s, C<sup>i</sup>iso Ph), 138.3 (s, C<sup>i</sup>iso Ph), 131.0 - 128.9 (s, C<sup>3.5</sup>H C<sub>5</sub>H<sub>3</sub>N, Ph), 97.3 (s, CH allyl), 82.0 (s, OCH<sub>2</sub>), 80.2 (s, OCH<sub>2</sub>), 69.6 (s, CHPh), 68.7 (s, CHPh), 43.1 (s, CH<sub>2</sub> allyl), 28.7 (s, CH<sub>2</sub> allyl) ppm; minor isomer,  $\delta$  173.4 (s, OCN), 173.2 (s, OCN), 145.2 (s, C<sup>2.6</sup> C<sub>5</sub>H<sub>3</sub>N), 145.1 (s, C<sup>2.6</sup> C<sub>5</sub>H<sub>3</sub>N), 141.7 (s, C<sup>4</sup>H C<sub>5</sub>H<sub>3</sub>N), 138.2 (s, C<sup>i</sup>iso Ph), 137.5 (s, C<sup>i</sup>iso Ph), 131.0 - 128.9 (C<sup>3.5</sup>H C<sub>5</sub>H<sub>3</sub>N, Ph), 94.0 (s, CH allyl), 81.0 (s, OCH<sub>2</sub>), 80.8 (s, OCH<sub>2</sub>), 70.2 (s, CHPh), 66.9 (s, CHPh), 44.4 (s, CH<sub>2</sub> allyl), 29.5 (s, CH<sub>2</sub> allyl) ppm. Anal. Calcd for C<sub>26</sub>H<sub>24</sub>N<sub>3</sub>ClF<sub>6</sub>IrO<sub>2</sub>P (783.12): C 39.88, H 3.09, N 5.37. Found: C 39.65, H 3.04, N 5.20. FAB-MS: *m/z* 638 [IrCl(C<sub>3</sub>H<sub>5</sub>)(Ph-pybox)]<sup>+</sup>.

**Synthesis of Complexes [IrCl<sub>3</sub>( $\kappa^3$ -*N,N,N*-R-pybox)] (R = <sup>i</sup>Pr (12), Ph (13)).** To a suspension of [Ir( $\mu$ -Cl)( $\eta^2$ -C<sub>8</sub>H<sub>14</sub>)<sub>2</sub>] (0.179 g, 0.2 mmol) in dichloromethane (3 mL) was added consecutively a saturated solution of Cl<sub>2</sub> in carbon tetrachloride (0.290 mL) and pybox (0.4 mmol). The resulting solution was stirred for 15 min, and the solvent was then removed under vacuum. The solid obtained was transferred to a silica gel chromatography column. Elution with a 10:1 dichloromethane/methanol mixture gave a dark fraction, from which complexes **12** and **13** were isolated after solvent evaporation.

**Complex 12.** Yield: 76% (0.182 g). Color: dark green. <sup>1</sup>H NMR (300 MHz, acetone-*d*<sub>6</sub>, 293 K):  $\delta$  8.19 (br s, 3H, H<sup>3.4.5</sup> C<sub>5</sub>H<sub>3</sub>N), 5.27 (m, 4H, OCH<sub>2</sub>), 4.40 (m, 2H, CH<sup>i</sup>Pr), 3.01 (m, 2H, CHMe<sub>2</sub>), 1.03 (s, 3H, CHMe<sub>2</sub>), 1.00 (s, 3H, CHMe<sub>2</sub>), 0.99 (s, 3H, CHMe<sub>2</sub>), 0.97 (s, 3H, CHMe<sub>2</sub>) ppm. <sup>13</sup>C{<sup>1</sup>H} NMR (75.4 MHz, acetone-*d*<sub>6</sub>, 293 K):  $\delta$  173.0 (s, OCN), 148.4 (s, C<sup>2.6</sup> C<sub>5</sub>H<sub>3</sub>N), 140.3 (s, C<sup>4</sup>H C<sub>5</sub>H<sub>3</sub>N), 127.7 (s, C<sup>3.5</sup>H C<sub>5</sub>H<sub>3</sub>N), 74.1 (s, OCH<sub>2</sub>), 69.9 (s, CH<sup>i</sup>Pr), 28.8 (s, CHMe<sub>2</sub>), 19.4 (s, CHMe<sub>2</sub>), 15.5 (s, CHMe<sub>2</sub>) ppm. Anal. Calcd for C<sub>17</sub>H<sub>23</sub>N<sub>3</sub>Cl<sub>3</sub>IrO<sub>2</sub>·Me<sub>2</sub>CO: C 36.50, H 4.44, N 6.39. Found: C 36.12, H 4.50, N 6.22. FAB-MS: *m/z* 564 [IrCl<sub>2</sub>(<sup>i</sup>Pr-pybox)]<sup>+</sup>, 529 [IrCl(<sup>i</sup>Pr-pybox)]<sup>+</sup>.

**Complex 13.** Yield: 78% (0.208 g). Color: dark yellow. <sup>1</sup>H NMR (400 MHz, CD<sub>2</sub>Cl<sub>2</sub>, 293 K):  $\delta$  8.00 (br s, 3H, H<sup>3.4.5</sup> C<sub>5</sub>H<sub>3</sub>N), 7.53, 7.36 (2  $\times$  m, 10H, Ph), 5.55 (m, 2H, OCH<sub>2</sub>), 5.42 (m, 2H, OCH<sub>2</sub>), 5.02 (pt,  $J_{\text{HH}} = 8.6$  Hz, 2H, CHPh) ppm. <sup>13</sup>C{<sup>1</sup>H} NMR (100.6 MHz, CD<sub>2</sub>Cl<sub>2</sub>, 293 K):  $\delta$  173.5 (s, OCN), 147.7 (s, C<sup>2.6</sup> C<sub>5</sub>H<sub>3</sub>N),

139.0 (s, C<sup>4</sup>H C<sub>5</sub>H<sub>3</sub>N), 136.6 (s, C<sup>ipso</sup> Ph), 128.7, 128.6, 128.3 (s, Ph), 127.2 (s, C<sup>3,5</sup>H C<sub>5</sub>H<sub>3</sub>N), 80.5 (s, OCH<sub>2</sub>), 67.8 (s, CHPh) ppm. Anal. Calcd for C<sub>23</sub>H<sub>19</sub>N<sub>3</sub>Cl<sub>3</sub>IrO<sub>2</sub>·Me<sub>2</sub>CO: C 43.01, H 3.47, N 5.79. Found: C 43.29, H 3.63, N 5.52.

**Synthesis of Complexes [IrCl<sub>2</sub>(κ<sup>3</sup>-N,N,N-R-pybox)(μ-Cl)M][Y] (R = <sup>i</sup>Pr, M = Ag, X = BF<sub>4</sub> (14a), SbF<sub>6</sub> (14b), M = Tl, X = PF<sub>6</sub> (14c); R = Ph, M = Ag, X = BF<sub>4</sub> (15a), SbF<sub>6</sub> (15b), M = Tl, X = PF<sub>6</sub> (15c)).** A solution of [IrCl<sub>3</sub>(κ<sup>3</sup>-N,N,N-R-pybox)] (R = <sup>i</sup>Pr, Ph) (0.5 mmol) in acetone (10 mL) was stirred for 1 h at room temperature (in the absence of light in the case of silver salts) with AgSbF<sub>6</sub> (0.344 g, 1 mmol), AgBF<sub>4</sub> (0.195 g, 1 mmol), or TlPF<sub>6</sub> (0.349, 1 mmol). The resulting red solution was filtered and concentrated to ca. 2 mL. Addition of diethyl ether afforded a red-orange solid, which was washed with diethyl ether (3 × 5 mL) and then vacuum-dried.

**Complex 14a.** [M] = Ag, Y = [BF<sub>4</sub>]. Yield: 95% (0.377 g). Color: red. IR (KBr, ν, cm<sup>-1</sup>): 1050 (BF<sub>4</sub><sup>-</sup>). Molar conductivity (acetone 20 °C, Ω<sup>-1</sup> cm<sup>2</sup> mol<sup>-1</sup>): 92. <sup>1</sup>H NMR (400 MHz, acetone-*d*<sub>6</sub>, 293 K): δ 8.41 (br, 3H, H<sup>3,4,5</sup> C<sub>5</sub>H<sub>3</sub>N), 5.37 (m, 4H, OCH<sub>2</sub>), 4.58 (m, 2H, CH<sup>i</sup>Pr), 2.86 (m, 2H, CHMe<sub>2</sub>), 1.06 (d, *J*<sub>HH</sub> = 7.1 Hz, 6H, CHMe<sub>2</sub>), 1.02 (d, *J*<sub>HH</sub> = 6.8 Hz, 6H, CHMe<sub>2</sub>) ppm. <sup>13</sup>C{<sup>1</sup>H} NMR (75.4 MHz, acetone-*d*<sub>6</sub>, 293 K): δ 173.4 (s, OCN), 148.2 (s, C<sup>2,6</sup> C<sub>5</sub>H<sub>3</sub>N), 142.7 (s, C<sup>4</sup>H C<sub>5</sub>H<sub>3</sub>N), 128.9 (s, C<sup>3,5</sup>H C<sub>5</sub>H<sub>3</sub>N), 74.6 (s, OCH<sub>2</sub>), 70.0 (s, CH<sup>i</sup>Pr), 29.6 (s, CHMe<sub>2</sub>), 19.4 (s, CHMe<sub>2</sub>), 15.4 (s, CHMe<sub>2</sub>) ppm. Anal. Calcd for C<sub>17</sub>H<sub>23</sub>N<sub>3</sub>AgBCl<sub>3</sub>F<sub>4</sub>IrO<sub>2</sub> (794.63): C 25.70, H 2.92, N 5.29. Found: C 25.45, H 3.01, N 5.19. ESI-MS: *m/z* 708 [IrCl<sub>3</sub>(<sup>i</sup>Pr-pybox)Ag]<sup>+</sup> (43%), 1307 [{IrCl<sub>3</sub>(<sup>i</sup>Pr-pybox)}<sub>2</sub>Ag]<sup>+</sup> (100%).

**Complex 14b.** [M] = Ag, Y = [SbF<sub>6</sub>]. Yield: 92% (0.434 g). Color: red. IR (KBr, ν, cm<sup>-1</sup>): 665 (SbF<sub>6</sub><sup>-</sup>). <sup>1</sup>H NMR (400 MHz, acetone-*d*<sub>6</sub>, 293 K): δ 8.39 (br, 3H, H<sup>3,4,5</sup> C<sub>5</sub>H<sub>3</sub>N), 5.37 (m, 4H, OCH<sub>2</sub>), 4.58 (m, 2H, CH<sup>i</sup>Pr), 2.86 (m, 2H, CHMe<sub>2</sub>), 1.06 (d, *J*<sub>HH</sub> = 7.1 Hz, 6H, CHMe<sub>2</sub>), 1.04 (d, *J*<sub>HH</sub> = 6.7 Hz, 6H, CHMe<sub>2</sub>) ppm. <sup>13</sup>C{<sup>1</sup>H} NMR (75.4 MHz, acetone-*d*<sub>6</sub>, 293 K): δ 173.3 (s, OCN), 148.0 (s, C<sup>2,6</sup> C<sub>5</sub>H<sub>3</sub>N), 143.0 (s, C<sup>4</sup>H C<sub>5</sub>H<sub>3</sub>N), 129.0 (s, C<sup>3,5</sup>H C<sub>5</sub>H<sub>3</sub>N), 74.4 (s, OCH<sub>2</sub>), 70.3 (s, CH<sup>i</sup>Pr), 29.9 (s, CHMe<sub>2</sub>), 19.3 (s, CHMe<sub>2</sub>), 15.3 (s, CHMe<sub>2</sub>) ppm. Anal. Calcd for C<sub>17</sub>H<sub>23</sub>N<sub>3</sub>AgCl<sub>3</sub>F<sub>6</sub>IrO<sub>2</sub>Sb (943.58): C 21.64, H 2.46, N 4.45. Found: C 21.42, H 2.42, N 4.50. ESI-MS: *m/z* 564 [IrCl<sub>2</sub>(<sup>i</sup>Pr-pybox)]<sup>+</sup> (100%). MALDI-MS: *m/z* 814 [IrCl<sub>3</sub>(<sup>i</sup>Pr-pybox)Ag<sub>2</sub> - 1]<sup>+</sup> (100%), 564 [IrCl<sub>2</sub>(<sup>i</sup>Pr-pybox)]<sup>+</sup> (70%).

**(14c).** [M] = Tl, Y = [PF<sub>6</sub>]. Yield: 94% (0.446 g). Color: red. IR (KBr, ν, cm<sup>-1</sup>): 846 (PF<sub>6</sub><sup>-</sup>). Molar conductivity (acetone 20 °C, Ω<sup>-1</sup> cm<sup>2</sup> mol<sup>-1</sup>): 70. <sup>1</sup>H NMR (400 MHz, acetone-*d*<sub>6</sub>, 293 K): δ 8.29 (br, 3H, H<sup>3,4,5</sup> C<sub>5</sub>H<sub>3</sub>N), 5.32 (m, 4H, OCH<sub>2</sub>), 4.58 (m, 2H, CH<sup>i</sup>Pr), 2.96 (m, 2H, CHMe<sub>2</sub>), 1.04 (d, *J*<sub>HH</sub> = 7.2 Hz, 6H, CHMe<sub>2</sub>), 1.02 (d, *J*<sub>HH</sub> = 6.8 Hz, 6H, CHMe<sub>2</sub>) ppm. <sup>13</sup>C{<sup>1</sup>H} NMR (100.6 MHz, acetone-*d*<sub>6</sub>, 293 K): δ 172.3 (s, OCN), 147.4 (s, C<sup>4</sup>H C<sub>5</sub>H<sub>3</sub>N), 140.8 (s, C<sup>2,6</sup> C<sub>5</sub>H<sub>3</sub>N), 127.7 (s, C<sup>3,5</sup>H C<sub>5</sub>H<sub>3</sub>N), 73.5 (s, OCH<sub>2</sub>), 69.2 (s, CH<sup>i</sup>Pr), 28.3 (s, CHMe<sub>2</sub>), 18.5 (s, CHMe<sub>2</sub>), 14.6 (s, CHMe<sub>2</sub>) ppm. Anal. Calcd for C<sub>17</sub>H<sub>23</sub>N<sub>3</sub>Cl<sub>3</sub>F<sub>6</sub>IrO<sub>2</sub>PTl (949.31): C 21.51, H 2.44, N 4.43. Found: C 21.83, H 2.47, N 4.41. ESI-MS: *m/z* 804 [IrCl<sub>3</sub>(<sup>i</sup>Pr-pybox)Tl]<sup>+</sup> (33%), 564 [IrCl<sub>2</sub>(<sup>i</sup>Pr-pybox)]<sup>+</sup> (100%).

**Complex 15a.** [M] = Ag, Y = [BF<sub>4</sub>]. Yield: 92% (0.397 g). Color: red. IR (KBr, ν, cm<sup>-1</sup>): 1063 (BF<sub>4</sub><sup>-</sup>). <sup>1</sup>H NMR (400 MHz, acetone-*d*<sub>6</sub>, 293 K): δ 8.54 (s, 3H, H<sup>3,4,5</sup> C<sub>5</sub>H<sub>3</sub>N), 7.69, 7.48 (2 × m, 10H, Ph), 5.89 (pt, *J*<sub>HH</sub> = 9.7 Hz, 2H, OCH<sub>2</sub>), 5.56 (pt, *J*<sub>HH</sub> = 9.7 Hz, 2H, OCH<sub>2</sub>), 5.32 (pt, *J*<sub>HH</sub> = 9.7 Hz, 2H, CHPh) ppm. <sup>13</sup>C{<sup>1</sup>H} NMR (75.4 MHz, acetone-*d*<sub>6</sub>, 293 K): δ 174.0 (s, OCN), 147.8 (s, C<sup>2,6</sup> C<sub>5</sub>H<sub>3</sub>N), 143.3 (s, C<sup>4</sup>H C<sub>5</sub>H<sub>3</sub>N), 137.3 (s, C<sup>ipso</sup> Ph), 130.2, 129.7, 129.6, 129.3, 129.0 (s, Ph), 127.6 (s, C<sup>3,5</sup>H C<sub>5</sub>H<sub>3</sub>N), 81.0 (s, OCH<sub>2</sub>), 68.2 (s, CHPh) ppm. Anal. Calcd for C<sub>23</sub>H<sub>19</sub>N<sub>3</sub>AgBCl<sub>3</sub>F<sub>4</sub>IrO<sub>2</sub> (862.66): C 32.02, H 2.22, N 4.87. Found: C 31.97, H 2.16, N 4.78. ESI-MS: *m/z* 776 [IrCl<sub>3</sub>(Ph-pybox)Ag]<sup>+</sup> (100%).

**Table 7. Crystal Data and Structure Refinement for 8 and 14c·Me<sub>2</sub>CO**

	8	14c·Me <sub>2</sub> CO
chem formula	C <sub>19</sub> H <sub>27</sub> F <sub>6</sub> I <sub>2</sub> IrN <sub>3</sub> O <sub>2</sub> P	C <sub>20</sub> H <sub>26</sub> Cl <sub>3</sub> F <sub>6</sub> IrN <sub>3</sub> O <sub>3</sub> PTl
fw	920.41	1007.35
<i>T</i> (K)	293(2)	150(2)
wavelength (Å)	0.71073	1.5418
cryst system	monoclinic	monoclinic
space group	<i>P</i> 2 <sub>1</sub>	<i>P</i> 2 <sub>1</sub>
<i>a</i> (Å)	7.7764(6)	10.1512(2)
<i>b</i> (Å)	17.4020(13)	11.4196(2)
<i>c</i> (Å)	9.3814(7)	12.8731(4)
β (deg)	91.4090(10)	98.977(1)
<i>V</i> (Å <sup>3</sup> )	1269.15(17)	1474.00(6)
<i>Z</i>	2	2
ρ <sub>calcd</sub> (g cm <sup>-3</sup> )	2.408	2.270
μ (mm <sup>-1</sup> )	7.822	22.610
<i>F</i> (000)	860	944
cryst size (mm)	0.28 × 0.26 × 0.24	0.15 × 0.1 × 0.05
θ range (deg)	2.17 to 28.08	5.17 to 69.77
index ranges	-9 ≤ <i>h</i> ≤ 10 -22 ≤ <i>k</i> ≤ 22 -12 ≤ <i>l</i> ≤ 9	-12 ≤ <i>h</i> ≤ 12 -13 ≤ <i>k</i> ≤ 13 0 ≤ <i>l</i> ≤ 15
no. of rflns collected	8647	24 938
no. of indep rflns	5614 [R(int) = 0.0319]	5424 [R(int) = 0.0907]
completeness to θ <sub>max</sub> , %	98.5	98.2
no. params/restraints	307/1	344/1
goodness-of-fit on <i>F</i> <sup>2</sup>	1.013	1.050
<i>R</i> [ <i>I</i> > 2σ( <i>I</i> )] <sup>a</sup>	<i>R</i> <sub>1</sub> = 0.0294, <i>wR</i> <sub>2</sub> = 0.0711	<i>R</i> <sub>1</sub> = 0.0485, <i>wR</i> <sub>2</sub> = 0.1221
<i>R</i> (all data)	<i>R</i> <sub>1</sub> = 0.0309, <i>wR</i> <sub>2</sub> = 0.0717	<i>R</i> <sub>1</sub> = 0.0507, <i>wR</i> <sub>2</sub> = 0.1268
absolute struct param	0.005(5)	-0.003(16)
largest diff peak and hole (e Å <sup>-3</sup> )	1.156 and -1.802	1.746 and -2.316

$$^a R_1 = \sum(|F_o| - |F_c|)/\sum|F_o|; wR_2 = \{\sum[w(F_o^2 - F_c^2)^2]/\sum[w(F_o^2)^2]\}^{1/2}.$$

**Complex 15b.** [M] = Ag, Y = [SbF<sub>6</sub>]. Yield: 93% (0.470 g). Color: red. IR (KBr, ν, cm<sup>-1</sup>): 660 (SbF<sub>6</sub><sup>-</sup>). <sup>1</sup>H NMR (300 MHz, acetone-*d*<sub>6</sub>, 293 K): δ 8.54 (s, 3H, H<sup>3,4,5</sup> C<sub>5</sub>H<sub>3</sub>N), 7.67, 7.45 (2 × m, 10H, Ph), 5.87 (pt, *J*<sub>HH</sub> = 9.8 Hz, 2H, OCH<sub>2</sub>), 5.53 (pt, *J*<sub>HH</sub> = 9.8 Hz, 2H, OCH<sub>2</sub>), 5.31 (pt, *J*<sub>HH</sub> = 9.8 Hz, 2H, CHPh) ppm. <sup>13</sup>C{<sup>1</sup>H} NMR (75.4 MHz, acetone-*d*<sub>6</sub>, 293 K): δ 173.6 (s, OCN), 147.5 (s, C<sup>2,6</sup> C<sub>5</sub>H<sub>3</sub>N), 142.5 (s, C<sup>4</sup>H C<sub>5</sub>H<sub>3</sub>N), 136.6 (s, C<sup>ipso</sup> Ph), 129.7, 129.3, 128.7 (s, Ph), 127.6 (s, C<sup>3,5</sup>H C<sub>5</sub>H<sub>3</sub>N), 80.6 (s, OCH<sub>2</sub>), 67.9 (s, CHPh) ppm. Anal. Calcd for C<sub>23</sub>H<sub>19</sub>N<sub>3</sub>AgCl<sub>3</sub>F<sub>6</sub>IrO<sub>2</sub>Sb (1011.61): C 27.31, H 1.89, N 4.15. Found: C 27.15, H 1.87, N 4.10.

**Complex 15c.** [M] = Tl, Y = [PF<sub>6</sub>]. Yield 96% (0.488 g). Color: orange. IR (KBr, ν, cm<sup>-1</sup>): 846 (PF<sub>6</sub><sup>-</sup>). Molar conductivity (acetone 20 °C, Ω<sup>-1</sup> cm<sup>2</sup> mol<sup>-1</sup>): 69. <sup>1</sup>H NMR (300 MHz, acetone-*d*<sub>6</sub>, 293 K): δ 8.45 (m, 3H, H<sup>3,4,5</sup> C<sub>5</sub>H<sub>3</sub>N), 7.62, 7.41 (2 × m, 10H, Ph), 5.82 (dd, *J*<sub>HH</sub> = 10.6 Hz, *J*<sub>HH</sub> = 9.3 Hz, 2H, OCH<sub>2</sub>), 5.54 (dd, *J*<sub>HH</sub> = 10.6 Hz, *J*<sub>HH</sub> = 8.8 Hz, 2H, OCH<sub>2</sub>), 5.20 (dd, *J*<sub>HH</sub> = 9.3 Hz, *J*<sub>HH</sub> = 8.8 Hz, 2H, CHPh) ppm. <sup>13</sup>C{<sup>1</sup>H} NMR (75.4 MHz, acetone-*d*<sub>6</sub>, 293 K): δ 176.2 (s, OCN), 149.9 (s, C<sup>2,6</sup> C<sub>5</sub>H<sub>3</sub>N), 142.9 (s, C<sup>4</sup>H C<sub>5</sub>H<sub>3</sub>N), 140.0 (s, C<sup>ipso</sup> Ph), 131.4, 131.1, 130.8, 130.5 (s, Ph and C<sup>3,5</sup>H C<sub>5</sub>H<sub>3</sub>N), 83.3 (s, OCH<sub>2</sub>), 70.1 (s, CHPh) ppm. Anal. Calcd for C<sub>23</sub>H<sub>19</sub>N<sub>3</sub>Cl<sub>3</sub>F<sub>6</sub>IrO<sub>2</sub>PTl (1017.34): C 27.15, H 1.88, N 4.13. Found: C 26.97, H 1.78, N 4.15. ESI-MS: *m/z* 872 [IrCl<sub>3</sub>(Ph-pybox)Tl]<sup>+</sup> (100%).

**General Procedure for Hydrogen Transfer Reactions.** The ketone (5 mmol) and the catalyst precursor (0.01 mmol) were placed in a three-neck Schlenk flask under a dry nitrogen atmosphere, and 2-propanol (50 mL) was added. The solution was heated at 82 °C for 15 min, and the corresponding amount of base from a 0.080 M solution in 2-propanol was added. The reaction was monitored by gas chromatography. The corresponding alcohol and acetone were the only products detected in all cases.

**X-Ray Crystal Structure Determination of Complexes 4 and 14c•Me<sub>2</sub>CO.** Crystals suitable for X-ray diffraction analysis were obtained by slow diffusion of diethyl ether into a saturated solution of complex **8** in dichloromethane or hexane into a saturated solution of complex **14c** in acetone. Complex **14c** crystallizes with a molecule of acetone. Data collection, crystal, and refinement parameters are collected in Table 7. Diffraction data for **8** were recorded at 293(2) K on a Bruker Smart CCD diffractometer using graphite-monochromated Mo K $\alpha$  radiation ( $\lambda = 0.71073$  Å). The data were collected using 0.3° wide  $\omega$  scans and a crystal-to-detector distance of 40 mm. The diffraction frames were integrated using the SAINT package<sup>17</sup> and corrected for absorption with SADABS.<sup>18</sup> Diffraction data for **14c**•Me<sub>2</sub>CO were recorded at 150(2) K on a Nonius KappaCCD single-crystal diffractometer using Cu K $\alpha$  radiation ( $\lambda = 1.5418$  Å). The crystal-to-detector distance was fixed at 29 mm, and the frames were collected using the oscillation method, with 2° oscillation and 40 s exposure time per frame. Data collection strategy for **8** and **14c**•Me<sub>2</sub>CO were calculated with the program Collect.<sup>19</sup> Data reduction and cell refinement were performed using the programs HKL Denzo and Scalepack.<sup>20</sup> Absorption correction was applied by means of SORTAV.<sup>21</sup>

The software package WINGX<sup>22</sup> was used for space group determination, structure solution, and refinement. The structures were solved by Patterson interpretation and phase expansion using DIRDIF.<sup>23</sup> Isotropic least-squares refinement on  $F^2$  using SHELXL-

97 was performed.<sup>24</sup> During the final stages all non-hydrogen atoms were refined with anisotropic displacement parameters (except the C9 atom of the <sup>i</sup>Pr-pybox ligand in **14c**•Me<sub>2</sub>CO; this disordered atom was found and isotropically refined). The H atoms were geometrically placed, and their coordinates were refined riding on their parent atoms. In both structures, the maximum residual electron density is located near heavier atoms. The function minimized was  $[\sum w(F_o^2 - F_c^2)/\sum w(F_o^2)]^{1/2}$ , where  $w = 1/[\sigma^2(F_o^2) + (aP)^2 + bP]$  ( $a = 0.0436$  and  $b = 0$  for **8**,  $a = 0.0917$  and  $b = 6.3768$  for **14c**•Me<sub>2</sub>CO), with  $\sigma(F_o^2)$  from counting statistics and  $P = (\max(F_o^2, 0) + 2F_c^2)/3$ . Atomic scattering factors were taken from the *International Tables for X-Ray Crystallography*.<sup>25</sup> Geometrical calculations were made with PARST.<sup>26</sup> The crystallographic plots were made with PLATON.<sup>27</sup>

**Acknowledgment.** This work was supported by the Ministerio de Educación y Ciencia of Spain (Projects BQU2003-00255 and MAT2006-01997, Consolider Ingenio 2010 (CSD2007-00006)) and Principado de Asturias (FICYT, Project PR-01-GE-4). P.P. thanks the Ministerio de Educación y Ciencia (MEC) of Spain for a Ph.D. fellowship.

**Supporting Information Available:** Crystallographic data for complexes **1**, **8**, **10**, and **14c**•Me<sub>2</sub>CO. Also, an X-ray crystallographic file in CIF format for the structure determination of complexes **1**, **8**, **10**, and **14c**•Me<sub>2</sub>CO. This material is available free of charge via the Internet at <http://pubs.acs.org>.

OM7011997

(17) SAINT version 6.02; Bruker Analytical X-ray Systems: Madison, WI, 2000.

(18) Sheldrick, G. M. *SADABS: Program for Empirical Absorption Correction*; University of Göttingen: Göttingen, Germany, 1996.

(19) Collect; Nonius BV: Delft, The Netherlands, 1997–2000.

(20) Otwinowski, Z.; Minor, W. *Methods Enzymol.* **1997**, 276, 307–326.

(21) Blessing, R. H. *Acta Crystallogr., Sect. A* **1995**, 51, 33–38.

(22) Farrugia, L. J. *J. Appl. Crystallogr.* **1999**, 32, 837–838.

(23) Beurskens, P. T.; Admiraal, G.; Beurskens, G.; Bosman, W. P.; García-Granda, S.; Gould, R. O.; Smits, J. M. M.; Smykalla, C. *The DIRDIF Program System*; Technical Report of the Crystallographic Laboratory; University of Nijmegen: Nijmegen, The Netherlands, 1999.

(24) Sheldrick, G. M. *SHELXL97: Program for the Refinement of Crystal Structures*; University of Göttingen: Göttingen, Germany, 1997.

(25) *International Tables for X-Ray Crystallography*; Kynoch Press: Birmingham, U.K., 1974; Vol. IV. (present distributor: Kluwer Academic Publishers, Dordrecht, The Netherlands).

(26) Nardelli, M. *Comput. Chem.* **1983**, 7, 95–98.

(27) Spek, A. L. *PLATON: A Multipurpose Crystallographic Tool*; University of Utrecht: Utrecht, The Netherlands, 2007.